JOURNAL OF GEOPHYSICAL RESEARCH, VOL. 95, NO. D4, PAGES 3473–3492, MARCH 20, 1990

Global Impact of the Antarctic Ozone Hole: Chemical Propagation

MICHAEL PRATHER AND ANDREW H. JAFFE[1]

NASA Goddard Space Flight Center, Institute for Space Studies, New York

A model is presented for the chemical mixing of stratospheric air over spatial scales from tens of kilometers to meters. Photochemistry, molecular diffusion, and strain (the stretching of air parcels due to wind shear) are combined into a single one-dimensional model. The model is applied to the case in which chemically perturbed air parcels from the Antarctic stratosphere are transported to mid-latitudes and strained into thin ribbon-like filaments until they are diffusively mixed with the ambient stratosphere. We find that the parcels may be treated as evolving in chemical isolation until the final mixing. When parcels reach a transverse thickness of 50-100 m in the lower stratosphere, they are rapidly dispersed by the combination of molecular diffusion and strain. The rapidity of the final mixing implies a lower limit to the vertical scales of inhomogeneities observed in the lower stratosphere. For this sensitivity study we consider four types of Antarctic air: a control case representing unprocessed polar air; heterogeneous processing by polar stratospheric clouds (PSCs) that has repartitioned the Cl_x and NO_y families; processing that also includes denitrification and dehydration; and all processing plus 90% ozone depletion. Large abundances of ClO, resulting initially from heterogeneous processing of stratospheric air on PSCs, are sustained by extensive denitrification. (One exception is the case of Antarctic air with major ozone depletion in which ClO is converted rapidly to HCl upon release of small amounts of NO_x as a result of the extremely nonlinear Cl_x-NO_y chemical system.) ClO concentrations in the mid-latitude stratosphere should be enhanced by as much as a factor of 5 due to the mixing of air processed around the Antarctic vortex and will remain elevated for most of the following season. Chemical propagation of the Antarctic ozone hole occurs in two phases: rapid loss of ozone in the heterogeneously processed parcels as they evolve in isolation, and more slowly, a relative recovery of ozone over the following months. Another important effect is the transport of denitrified Antarctic air reducing NO_x and hence the total catalytic destruction of ozone throughout the southern mid-latitudes. In Antarctic air that has already been depleted of ozone within the vortex, little additional loss occurs during transport, and the propagation of chemically perturbed air acts partially to offset the deficit at mid-latitudes caused by dynamical dilution of the ozone hole. In air which has not experienced substantial ozone loss, chemical propagation can generate a net ozone deficit of order 2-3% at mid-latitudes.

1. INTRODUCTION

The appearance of a hole in the stratospheric ozone layer over Antarctica [*Farman et al.*, 1985; *Stolarski et al.*, 1986] has prompted a range of theoretical investigations on the origin of this phenomenon and its implications for ozone globally. In particular, questions have been asked about the impact of this ozone deficit throughout the southern hemisphere following the breakdown in late spring of the Antarctic circumpolar winds that define the winter vortex. Another important issue is whether the chemical processes responsible for generating the ozone hole extend beyond the vortex thereby contributing to ozone loss at mid-latitudes in early spring. Several studies using two- and three-dimensional chemical transport models have shown that following the chemical generation of an ozone deficit within the polar vortex, the ozone depletion is dispersed to southern mid-latitudes before it can be filled in by photochemical regeneration [*Polar Ozone Workshop*, 1988; *Sze et al.*, 1989; *Prather et al.*, 1990; *Chipperfield and Pyle*, 1988].

Chemical abundances in the Antarctic stratosphere are highly perturbed by the end of winter [*Keys et al.*, 1986; *Solomon et al.*, 1987; *de Zafra et al.*, 1987; *Anderson et al.*, 1988; *Polar Ozone Workshop*, 1988]; in particular, much of the chlorine has been converted to highly reactive forms such as ClO. Air parcels from the Antarctic lower stratosphere that are spun off from the vortex and reach mid-latitudes therefore contain not only an ozone deficit but also significant perturbations to the chlorine and odd-nitrogen compounds. The persistence of this chemical signature in these parcels, and the manner in which air parcels mix with the ambient air at mid-latitudes, will control the rate of ozone destruction following the breakup of the Antarctic vortex. If the parcel is mixed rapidly with ambient air, then catalytic chlorine cycles that destroy ozone would be shut down; if, however, the parcel remains isolated chemically at mid-latitudes, ozone loss may continue.

We present here a model for the chemical mixing of stratospheric air that combines photochemistry, molecular diffusion, and strain (i.e., the stretching of air parcels due to wind shear). These three processes can be represented by a high resolution, one-dimensional model with a grid scale of 10 m. Strain is responsible for reducing the size of the parcel from its initial scale of several kilometers in the vertical by several hundred kilometers in the horizontal. Diffusion is responsible for the final mixing with ambient air. This process is shown to occur rapidly when the parcel reaches dimensions of 100 m or less in vertical extent, and thus these scales should be the smallest vertical structures of inhomogeneous composition observable in the lower stratosphere. The spatial resolution of studies using global models is insufficient to follow the chemically perturbed air until it is mixed; specifically, the global models must assume that everything is

[1]Now at Department of Astronomy and Astrophysics, University of Chicago, Chicago, IL.

Paper number 89JD02940.
0148-0227/90/89JD-02940$05.00

mixed on the smallest scale resolved by the model, typically greater than 2 km vertically and 1000 km horizontally.

Perturbations to stratospheric chemistry over Antarctica are associated with reactions on polar stratospheric clouds (PSCs, see *McCormick and Trepte* [1986]): chlorine is converted to reactive forms, and sometimes water vapor and odd nitrogen are both removed by precipitation [*Toon et al.*, 1986; *Molina et al.*, 1987; *Wofsy et al.*, 1988]. Within the dynamically isolated vortex, sunlight drives chemical reactions involving ClO and BrO and can deplete local ozone abundances by as much as 90% [*Molina and Molina*, 1986; *Hofmann et al.*, 1987; *McElroy and Salawitch*, 1989]. In addition, these chemical perturbations are mixed into the mid-latitudes by air "peeling off" the vortex [*Juckes and McIntyre*, 1987] and may lead to later photochemical loss of ozone outside of the vortex.

The magnitude of ozone depletion within the vortex depends on details of the chemical perturbation, particularly denitrification [*Salawitch et al.*, 1988]. In our model the extent of denitrification controls the time scale for photochemical recovery in the air parcels spun out from the vortex. The catalytic destruction of ozone is driven by high concentrations of ClO; the process is terminated either by this photochemical recovery or by diffusive mixing with unperturbed air. Additional photochemical loss of ozone at mid-latitudes is greatest for those parcels that have been chemically processed by PSCs but transported to mid-latitudes before experiencing the large depletions associated with the Antarctic ozone hole. This in situ loss of ozone complements the depletion of ozone at southern mid-latitudes that occurs when ozone-poor air from within the Antarctic vortex is dynamically diluted into the mid-latitude stratosphere. We examine here this chemical propagation of the Antarctic ozone hole.

In section 2 we present the model for strain and diffusion, showing examples for an inert tracer. In section 3 we document the photochemical model, give examples of the evolution of perturbed chemistries within an isolated air parcel, and examine the chemical interface that develops between perturbed and ambient air. In section 4 we summarize our results and discuss the implications for widespread ozone loss due to the propagation of perturbed chemistry associated with the winter polar stratosphere.

2. Model for Strain and Diffusion

Within a fluid an arbitrarily defined volume, such as a parcel of air molecules in the atmosphere, is subjected to the effects of at least two dynamical processes on vastly differing scales: the almost random straining or stretching of the fluid volume due to bulk motions, and true mixing with the neighboring fluid due to diffusive processes such as molecular diffusion [*Batchelor*, 1959; *Kraichnan*, 1974]. We have created a one-dimensional model that combines these two processes and is easily integrable into our photochemical model.

2.1. *Random Strain*

Wind shear is an elementary notion from fluid dynamics. If there is a velocity gradient in the wind field, then any initial structure in the atmosphere will be stretched out in a direction perpendicular to the gradient. The shorter dimensions of the structure will decay inversely with time. However, wind fields in the atmosphere are not static; the direction and amplitude of winds are constantly changing on all spatial scales.

In order to handle realistic wind fields, the concept of strain must be introduced. We no longer must know the structure of the wind field relative to the orientation of the fluid parcel, but instead require that the velocity field changes in a quasi-random manner over the space and time scales of interest (i.e., the "white noise" field of *Kraichnan* [1974]). The theory of random straining in a fluid states that the decay of the shortest dimension of a parcel is approximately exponential with time [*Batchelor*, 1959; *Kraichnan*, 1974].

The atmospheric strain rate, S (s^{-1}), which determines the stretching of an air parcel depends on details of the wind field and air parcels, and cannot be derived simply from knowledge of the general circulation. One estimate of the value of S may be made from the observed shear of the zonally averaged wind, typically 10^{-3} s^{-1} (i.e., a change of 10 m/s over 10 km in altitude). If such a large value were typical of random strain on all scales, then chemically distinct air parcels would rapidly thin to sizes below any measurable threshold in less than a day; however, this large shear is most effective in stretching the planetary scale dimensions of a parcel. The vertical gradient of the zonal wind does not produce a random strain with exponential decay of parcel thickness, but rather leads to thinning of parcels with a geometric limit: a parcel of indefinite vertical extent and a horizontal scale of 1000 km will be stretched rapidly to a thickness of 5 km in 2 days, but will take 10 days to reach a thickness of 1 km. Therefore a uniform wind shear can rapidly reduce planetary-scale features, but random strain in the wind field is necessary to reduce further parcel sizes.

Random strain in the wind field is expected to occur on all scales due to the interaction of wind shears in the vertical and horizontal and other turbulent processes that lead to irreversible deformation and thinning of air parcels (e.g., two-dimensional turbulence on isentropic surfaces [*McIntyre*, 1988; *Juckes and McIntyre*, 1987]). From numerical models [*Juckes and McIntyre*, 1987], the e-folding time for decay of the smallest dimension of air parcels (i.e., $1/S$) is found to be less than a few days in the lower stratosphere; however, this model is two dimensional and does not resolve the vertical. In this paper we adopt the value, $S = 10^{-5}$ s^{-1}, for most calculations.

A compact parcel of air, defined, for example, by high concentrations of a passive tracer, will be stretched out into a convoluted ribbon-like structure [*Batchelor*, 1952; *Welander*, 1955; *Kraichnan*, 1974; *Juckes and McIntyre*, 1987] whose minimum dimension decays as $\exp(-St)$. The detailed shape of the final structure is irrelevant. The strain-induced transformation conserves mass, and hence the distorted parcel may be treated as a large surface area with a thickness equal to the minimum dimension, e.g., a ribbon. It is across the surface of this ribbon that irreversible diffusive mixing occurs, resulting in the loss of the identity of the original air parcel.

We construct a one-dimensional model for the strain of air parcels by choosing the axis along the minimum dimension of the parcel and assuming that volume is conserved by expanding the surface area of the ribbon in the other (unresolved) dimensions. Diffusion (discussed in the next section) is effective only across this surface, that is, along the one dimension we are modeling. We choose a uniform grid with spacing Δz (in centimeters) denoted by

$$z_i = i\,\Delta z \quad \text{for } i = 1 \text{ to } N \tag{1}$$

Concentrations of a tracer, c_i, are defined at each point z_i. A

perturbed parcel is defined by a set of points having values of c_i different from the ambient air, represented by the surrounding grid points. During the calculation the length of the grid contracts with time as

$$\Delta z(t) = \Delta z(0) \exp(-St) \quad (2)$$

The mass of air associated with a given grid point, however, remains constant since the area perpendicular to the grid must increase proportionally. The integrated effects of chemistry or diffusion over the entire volume (parcel plus ambient) can be calculated using equal weighting for the grid points over all times.

2.2. *Molecular Diffusion*

The strain model presented above is dimensionless and becomes interesting only when physical processes of a given scale, such as molecular diffusion, cause interaction between adjacent grid points in the thinning parcel. The diffusion equation relating the concentrations is

$$\partial c/\partial t = D\, \partial^2 c/\partial z^2 \quad (3)$$

where D is the diffusion coefficient (in square centimeters per second). We couple the strain and diffusion processes by solving the implicit diffusion relation

$$c_i(t) = c_i(t-\Delta t) + [c_{i-1}(t) - 2c_i(t) + c_{i+1}(t)]\, D\, \Delta t / \Delta z(t)^2 \quad (4)$$

noting that Δz changes with time (equation (2)). For boundary conditions we assume that the tracer gradient is zero at the endpoints (i=1, i=N).

Under atmospheric conditions, molecular diffusion is likely to be the most important final process contributing to the irreversible mixing of chemically distinct air parcels. Values for the diffusion coefficients of common gases are available and range from 1 to 100 $cm^2\ s^{-1}$ under stratospheric temperatures and densities [*Mason and Marrero*, 1970]. Figure 1 shows examples of D for the diffusion of several molecules through air as a function of altitude in the mid-latitude stratosphere. Data for most atmospheric species, especially for the chemically reactive radicals, are lacking. For this study we focus on altitudes centering on the Antarctic ozone hole, about 20 km or 50 mbar, where most values of D cluster around 3.5 $cm^2\ s^{-1}$. In most of the following calculations we assume a uniform value of D for all species but also present cases with slower diffusion rates for larger molecules.

2.3. *Combined Strain-Diffusion Model*

Strain is the most important process acting on a chemically perturbed air parcel until the smallest dimension thins sufficiently so that molecular diffusion becomes dominant. In our calculations the process of mixing passes from a strain-dominated regime to a diffusion-dominated regime. While diffusion occurs continuously across the interface between two air parcels, the random strain sharpens the gradients that have been smoothed by molecular diffusion, nullifying its effects. We present here results from the combined strain-diffusion model for the mixing of an air parcel containing elevated concentrations of a passive tracer.

We initialize the model with the concentration of tracer c = 1.0 within a parcel and zero outside. The parcel begins as a layer of thickness 10^4 m and is represented by 25 out of 1000 grid points (see discussion on strain and wind shear in section 2.1). Figure 2 shows the profile of tracer concentration for D = 3.5 and 35 $cm^2\ s^{-1}$, using a strain rate of $10^{-5}\ s^{-1}$. The scale shown in Figure 2 highlights the final days, beginning with day number 6, in which the parcel may still be identified as distinct from the background. The final dispersion of the parcel into the surrounding air is a rapid process, taking about 4 days for the peak concentration within the parcel to drop from greater than 95% to less than 10% above background. This time interval is independent of D in these calculations but occurs at different spatial scales depending on the value: about 20 m for D = 3.5 $cm^2\ s^{-1}$, and 60 m for D = 35 $cm^2\ s^{-1}$.

We define as a diagnostic the full width of the pulse at c = 0.9 (FW90; note that after FW90 drops to zero, the pulse

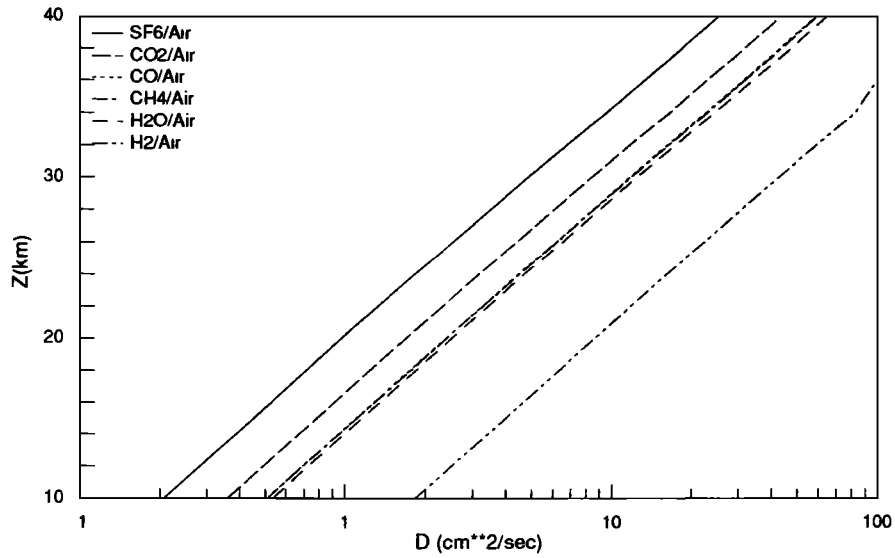

Fig. 1. Molecular diffusion coefficients ($cm^2\ s^{-1}$) in air for various gases as a function of altitude in the mid-latitude stratosphere.

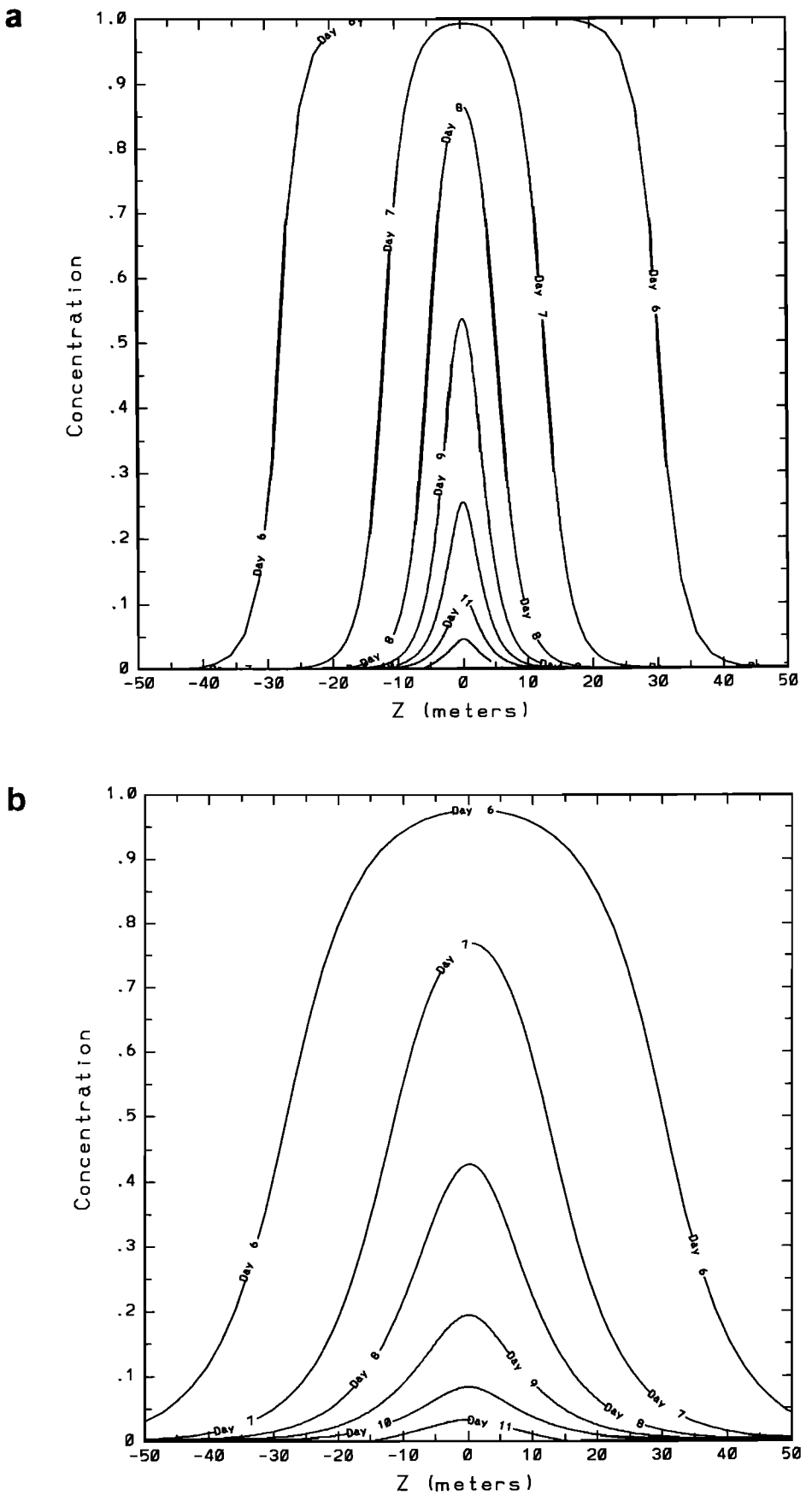

Fig. 2. The profile of a conservative tracer under the influence of both strain and diffusion, with strain parameter $S = 10^{-5}$ s^{-1}, and (*a*) diffusion coefficient $D = 3.5$ cm^2 s^{-1} and (*b*) $D = 35$ cm^2 s^{-1}. The pulse has an initial thickness of 10 km and a concentration of 1.

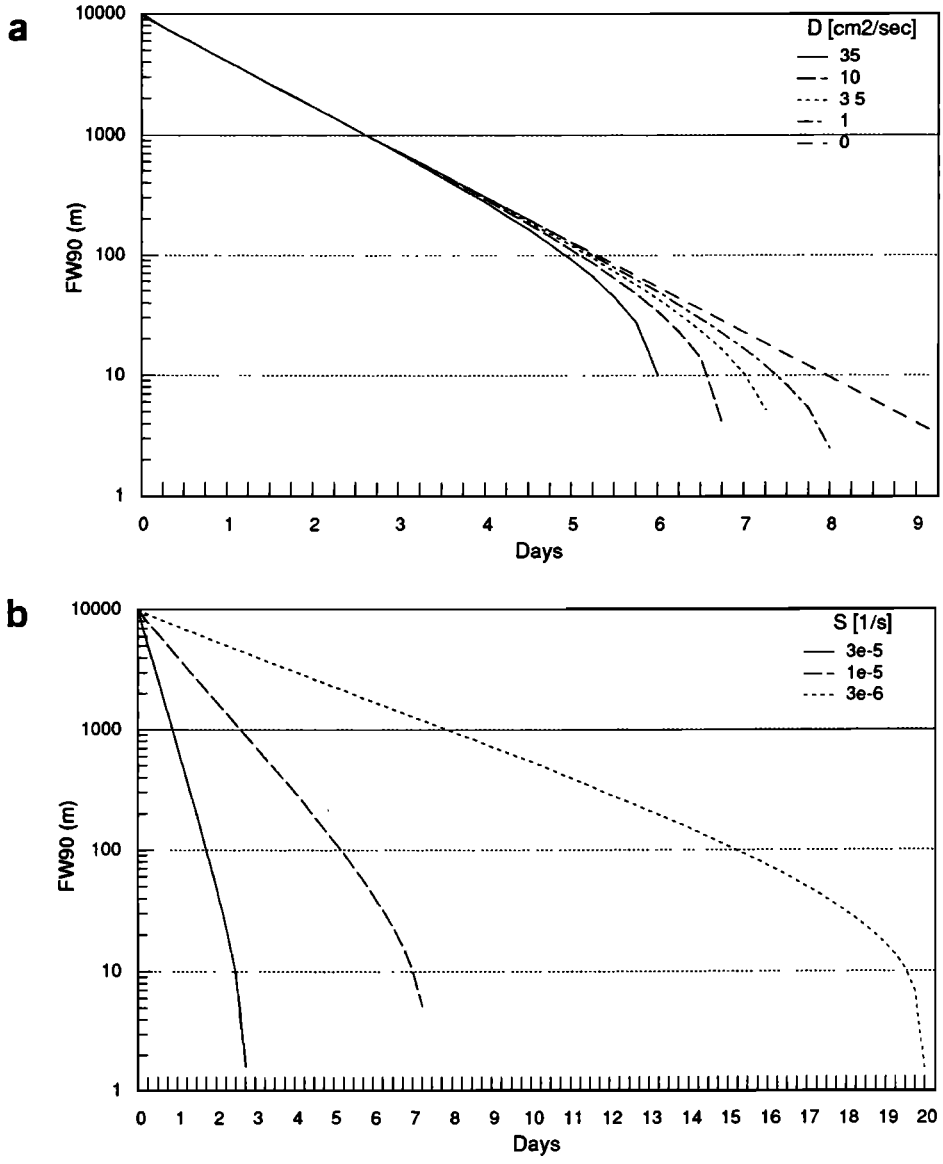

Fig. 3. Temporal evolution of the full width of a parcel at 90% of initial concentration (FW90; see text). The computation is shown for (*a*) a strain rate $S = 10^{-5}$ s^{-1} and several values of the diffusion coefficient, and for (*b*) a diffusion coefficient $D = 3.5$ cm^2 s^{-1} and several values of the strain rate.

is still identifiable for the following 4 days, see Figure 2). In Figure 3 we plot the logarithm of FW90 as a function of time in days from the initialization, varying D in Figure 3*a* and S in Figure 3*b*. The random strain acting alone produces a straight line equivalent to exponential decay with rate S (equation (2)). When diffusion becomes significant, the curve begins to depart from a straight line, and the value of FW90 decays more rapidly than an exponential. This point is clearly visible for each curve in Figure 3 and occurs at specific values of the parcel width for different values of D (Figure 3*a*) but is almost independent of S (Figure 3*b*). Diffusion alone cannot rapidly disperse the air parcels during this final stage without the simultaneous and continuing action of random strain.

For most of the lifetime of the parcel, very little mixing occurs with the ambient air, and chemical perturbations initially associated with the parcel remain intact. Calculations show that diffusive mixing with the background air is unimportant until the limiting diffusion length is reached, whereupon the parcel is rapidly absorbed. For example, during the first 7 days of the simulation shown in Figure 2*a*, 90% of the parcel's tracer has concentrations, $c > 0.5$; in the following 2 days this percentile drops to zero.

In the stratosphere a parcel of chemically perturbed air that is "peeled off" from the polar vortex is expected to have dimensions on the scale of planetary waves or synoptic-scale weather systems: a few kilometers in the vertical and several hundred kilometers horizontally. Horizontal scales are typically about 100 times greater than the corresponding vertical ones [*Holton*, 1979; *Juckes and McIntyre*, 1987]. As the parcel is stretched into a ribbon, the ratio of horizontal to vertical dimensions is expected to remain constant at first. On smaller scales, strain associated with gravity waves and turbulence is not expected to maintain this 100:1 aspect ratio, and thus air parcels reduced to vertical thicknesses of 50 m may have coherent horizontal extents of less than 1 km. However, the final diffusive mixing of the parcel will occur by

molecular diffusion acting most probably in the vertical direction [*Juckes and McIntyre*, 1987].

An obvious consequence of the random strain model is that one might expect to observe air parcels of different sizes at a frequency inversely proportional to their minimum dimension, because of the uniform exponential decay of scale size and the conservation of volume. The presence of diffusion, and hence the rapid decay of small scales, presents a cutoff to the size distribution of identifiable parcels. In model calculations shown in Figure 3, this limiting length scale varies from 50 to 200 m as a function of D and at a pressure of 50 mbar would correspond to parcels of order 60 m (vertical) by 6 km (horizontal). The rapid dispersion of smaller parcels may explain the minimum vertical structures of heterogeneity seen in the lower stratosphere [*NASA–WMO*, 1986, p. 459, pp. 963–966]. As the rate of molecular diffusion increases in the upper stratosphere, this theory predicts that the minimum size of vertical structures should be larger, as much as several hundred meters.

3. Perturbed Chemistry and the Evolution of Air Parcels

3.1. *The Photochemical Model*

The photochemical model used in these calculations has been documented at various stages over the past decade [*Logan et al.*, 1978; *Logan et al.*, 1981; *Prather et al.*, 1984]. The current version has been updated using JPL–87 rates [*DeMore et al.*, 1987] and more recent kinetic data for the ClO dimer (Cl_2O_2), OClO, BrCl and the ClO+BrO reaction. See Table 1 for the complete list of chemical species and the updates since JPL–87. The model does not include transport; it is nondimensional, solving the coupled set of chemical equations for all rapidly varying species over the diurnal cycle,

$$\partial c/\partial t = P - L \qquad (5)$$

where the net production rate (P–L) is composed of production and loss rates, respectively.

Kinetic rate coefficients are calculated from the local temperature and density, which are taken from climatological mean data for each latitude band (10° intervals) and month (NMC temperatures: R. D. McPeters, private communication, 1988). Photolysis rates are now calculated with (1) temperature-dependent absorption by molecular oxygen in the Schumann-Runge bands [*Fang et al.*, 1974], (2) use of climatological mean profiles for ozone and temperature [*McPeters et al.*, 1984], (3) fully spherical attenuation of sunlight with a plane-parallel Rayleigh-scattering atmosphere [*Prather*, 1974], and (4) twilight photolysis for solar zenith angles up to 96°.

For the rapidly varying species in Table 1, we solve equation (5) implicitly for variable time steps via a backward-Euler integration of the coupled differential equations, beginning and ending at noon each day. The time steps are typically 10 to 100 min and have finest resolution about sunset and sunrise when variations are most rapid. The more slowly varying species are not included in the implicit matrix, and their changes are computed with a standard forward-Euler integration of equation (5) over a 24-hour time step, using the diurnally averaged net production. Ozone, which can be integrated either implicitly or explicitly, is here calculated explicitly since in the lower stratosphere it varies little over the day. The chemical integration of an air parcel can be computed over consecutive diurnal cycles, or a parallel series of diurnal calculations can be used to force a photochemical steady state such that the diurnal cycle of each species repeats from day to day.

3.2. *Heterogeneous Processing*

We do not attempt in this paper to model directly the heterogeneous chemical processing of air in the polar vortex. Instead, we consider a range of chemical perturbations based upon observations from the Airborne Antarctic Ozone Experiment (AAOE) campaign and the theoretical work of others.

During winter, air within the polar stratospheric vortex is exposed to cold temperatures, in which various condensates are observed to form PSCs [*McCormick and Trepte*, 1986; *Hamill et al.*, 1988; *Hanson and Mauersberger*, 1988]. We now believe that this air is processed through heterogeneous chemical reactions on the cloud droplets or ice particles [*Molina et al.*, 1987; *Wofsy et al.*, 1988; *Tolbert et al.*, 1988; *Douglass and Stolarski*, 1989]. The impact of chemical transformations may range from conversion of N_2O_5 and $ClONO_2$ into HNO_3 and HOCl, to the removal of odd nitrogen and water through precipitation, and to the photochemical loss of O_3 associated with the Antarctic ozone hole. Much of this processing occurs on scales small compared to the size of the vortex in the neighborhood of a cloud, but is likely to become mixed over the spring season. For the purposes of this study, however, we treat the lower Antarctic stratosphere as a chemically distinct, homogeneous volume of air, in accord with AAOE observations of the chemically perturbed region [*Polar Ozone Workshop*, 1988].

The model for strain and diffusion presented in section 2 demonstrates that a chemically distinct air parcel may be treated in isolation until its final, diffusive mixing with ambient air. The duration of this isolation depends on the rate of random strain, which for values discussed here yields mixdown times of 5 to 20 days. In this section we follow the chemical evolution of heterogeneously processed stratospheric air, assuming that the parcel originated from within the Antarctic vortex and was dispersed rapidly to mid-latitudes by large-scale atmospheric motions. We define arbitrarily a sequence for the chemical perturbations to Antarctic air: (0), initial Antarctic conditions; (1), conversion of 99% of all NO_y, Cl_x, and Br_x species into HNO_3, ClO, and BrO; (2), heterogeneous conversion plus denitrification and dehydration of the parcel, removing 75% of NO_y and H_2O; (3), photochemical loss of 90% of the original ozone, in addition to processes (1) and (2).

The initial volume mixing ratios for the chemical families and other key long-lived species are based on observations [*NASA–WMO*, 1986] (see Table 1); the abundances of NO_y, Cl_x, Br_x, and other stable gases were not allowed to evolve during the integration of the parcel. Abundances of individual members of the chemical families were initialized from steady state calculations for Antarctic conditions in late spring. The steady state solutions leave the ozone concentration fixed at 3.5 ppm (parts per million by volume) based on observations, a value which is well above photochemical steady state.

3.3. *Photochemical Evolution*

A parcel of Antarctic air is relocated to 45°S on November 1 and allowed to evolve in isolation for 20 days. This

TABLE 1. The Photochemical Model

Chemical Family	Initialization at 75°S	Implicitly Integrated Chemical Species
O_x	3.5 ppm	$O(^3P)$, $O(^1D)$, O_3
HO_x	steady state	H, OH, HO_2, H_2O_2
RO_x	steady state	H_2CO, CH_3OO, CH_3OOH
NO_y	8.0 ppb	N, NO, NO_2, NO_3, N_2O_5[a], HNO_2, HNO_3[a], HO_2NO_2[a], $ClONO_2$[a], $BrONO_2$[a]
Cl_x	2.5 ppb	HCl, Cl, Cl_2, ClO, HOCl, OClO, Cl_2O_2, ($ClONO_2$[a]), BrCl
Br_x	14 ppt	BrO, Br, HBr, HOBr, ($BrONO_2$[a]), (BrCl)

Kinetic Data,[b] $k = A \exp(-B/T)$	A[b]	B,[b] °K	References
$BrO + ClO \rightarrow BrCl + O_2$	5.8×10^{-12} [cm^3 $molec^{-1}$ s^{-1}]	-168	*Sander and Friedl*
$\rightarrow Br + Cl + O_2$[c]	2.9×10^{-12}	-217	[1988]
$\rightarrow Br + OClO$	1.6×10^{-12}	-426	
$ClO + ClO \rightarrow Cl_2O_2$ (+M)	5.5×10^{-32} [cm^6 $molec^{-1}$ s^{-1}]	0	*Hayman et al.* [1988][d]
$Cl_2O_2 \rightarrow ClO + ClO$	1.26×10^{-26} [cm^{-3} molec]	8600	JPL–87

Cross Sections[b]	References[b]
OClO	*Wahner et al.* [1987]
Cl_2O_2[e]	*Cox and Hayman* [1988]; *Burkholder* [1988]
BrCl	Assumed to be 10 times the rate for Cl_2

Explicitly integrated, long-lived species and their assumed mixing ratios are CH_4 (1.0 ppm), C_2H_6 (30 ppt), CO (20 ppb), H_2O (4.0 ppm), H_2 (0.5 ppm), N_2O, $CFCl_3$, CF_2Cl_2, CCl_4, CH_3CCl_3, CH_3Cl, CH_3Br. Ozone can be treated either implicitly or explicitly (as O_x) depending upon the magnitude of its diurnal variation.

[a] Denotes species that were chosen to diffuse slowly in one experiment.

[b] Revisions since NASA JPL–87 [*DeMore et al.*, 1987], which is the basic reference for kinetic and photochemical data.

[c] ClOO produced by the reaction BrO + ClO is assumed to dissociate thermally to Cl + O_2.

[d] Cl_2O_2 rate coefficients [*Hayman et al.* 1988] have been adjusted by a factor of 0.4 at 200 K, reflecting the more recent work of *Sander et al.* [1989].

[e] Cl_2O_2 cross sections are based on *Cox and Hayman* [1988], but include the long-wavelength cross sections from 340 to 420 nm reported by *Burkholder* [1988].

assumption merely relocates the air parcel and does not attempt to follow any individual parcel's history of temperature and radiation from 75°S to 45°S. Figure 4*a* shows O_3 concentrations as a function of time for the control run (no heterogeneous processing) and for cases 1–3. The control (case 0) is not in steady state and shows a linear decline in O_3 of 0.14% per day; this decrease is expected for much of the lower stratosphere at mid-latitudes where net chemical loss is balanced by transport.

The initial (heterogeneous) release of ClO from the reservoir species of HCl and $ClONO_2$ results in rapid loss of O_x by catalytic cycles involving the ClO dimer and the reaction BrO + ClO. In these calculations, ozone loss through the Cl_2O_2 catalytic cycle is reduced compared to polar conditions because the warmer temperatures at mid-latitudes lead to more rapid thermal dissociation of the dimer. Photolysis of HNO_3 gradually releases NO_2 which ties up ClO in the form of $ClONO_2$. Loss of ozone is rapid initially, returning to a more normal rate of decline after 12 days in case 1, but continuing beyond 20 days in case 2 where denitrification has inhibited NO_2 release and ClO concentrations remain high. Air in which substantial O_3 depletion has already occurred (case 3) also experiences rapid initial loss, but in this case shows photochemical recovery with O_3 increasing after 5 days. In these calculations there is net loss of O_3 after 20 days for all cases: in the control (case 0) O_3 decreases by 0.1 ppm; in case 1, by 0.5 ppm; in case 2, by 1.3 ppm; and in case 3 ozone declines from an initial value of 0.35 ppm to 0.24 ppm. Thus air that has already experienced large photochemical depletion of O_3 over Antarctica (case 3) does not undergo much further loss when transported to mid-latitudes. On the other hand, air that has been chemically primed, but not exposed to sufficient sunlight to deplete the ozone over Antarctica, will experience significant ozone loss at mid-latitudes.

Figure 4*b* shows the evolution of NO_x partitioning, the ratio $(NO+NO_2)/NO_y$, for the four cases. In the control case 0, the ratio drops immediately from 0.22 and approaches the new steady state limit of 0.18 that corresponds to the sunlight and temperature conditions at 45°S. For cases 1–3 the concentration of NO_x grows following its initial heterogeneous removal; high levels of ClO force most of the NO_x to be stored as $ClONO_2$ (see discussion of Cl_x family below). Under these conditions, NO_x and ClO are titrated against each other, with $ClONO_2$ as the reservoir species, a case similar to that for multiple solutions found in the lower stratosphere [*Prather et*

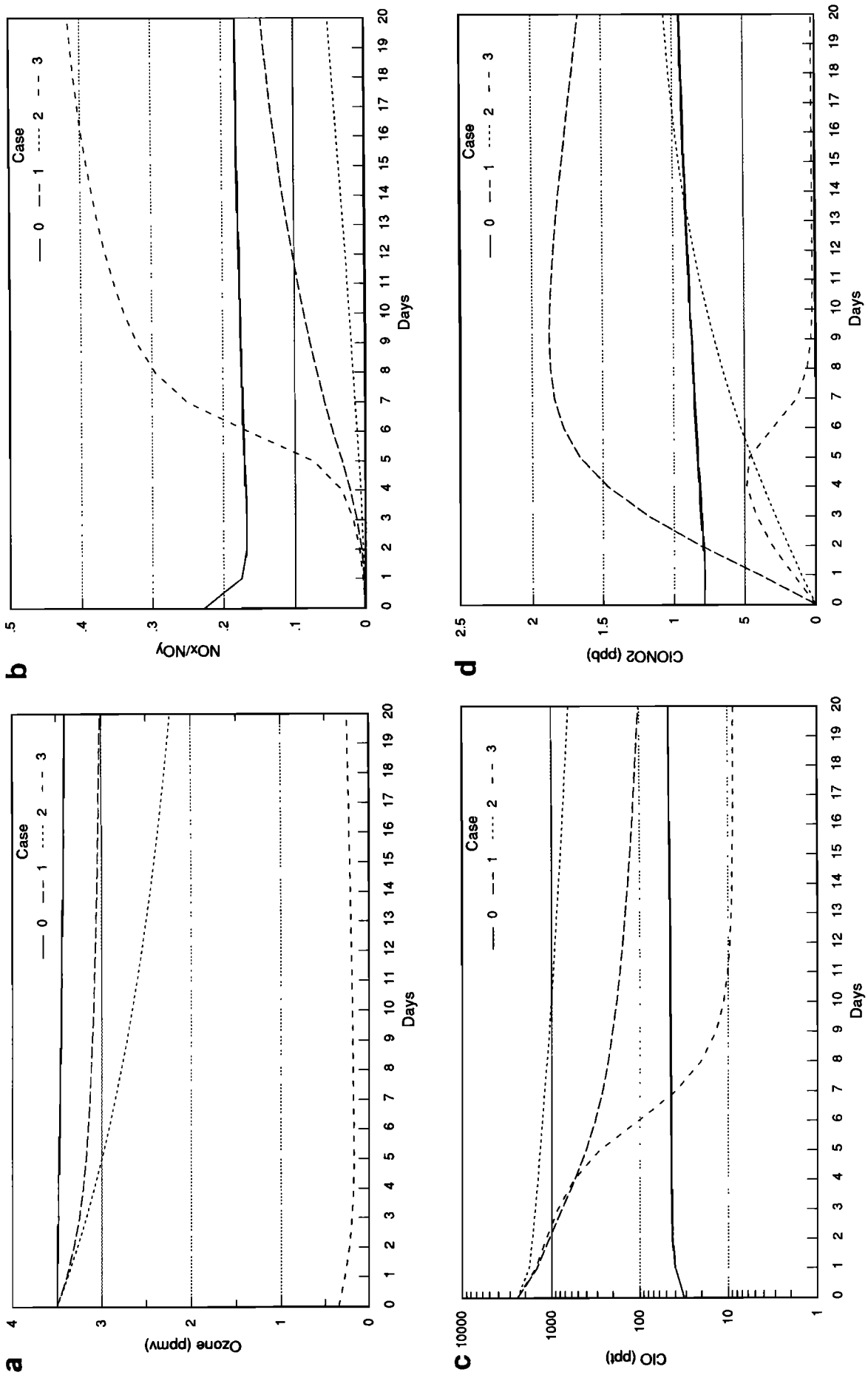

Fig. 4. Temporal evolution of chemical species for the four test cases (labeled 0, 1, 2, 3) after the parcel is moved from 75°S to 45°S. Results are shown for (*a*) ozone, (*b*) the ratio NO_x/NO_y, (*c*) ClO, and (*d*) $ClONO_2$. Case 0 represents unprocessed polar air; in case 1 heterogeneous processing by PSCs has repartitioned the Cl_x and NO_y families; in case 2 the air has also been denitrified and dehydrated; and case 3 further assumes that 90% of the ozone has been lost within the vortex.

al., 1979]. Mixing ratios of NO_x remain suppressed until the amount released by photolysis of HNO_3 exceeds the amount of ClO formed by the heterogeneous processing. Recovery of NO_x takes longer when denitrification has occurred (case 2 versus case 1). With large ozone loss (case 3) the evolution of NO_x is quite unusual: it is partitioned predominantly in the form of NO because O_3 levels are so low; NO_x concentrations grow rapidly after day 4 and approach steady state values; the sudden rise corresponds to the rapid drop in ClO concentrations (see below). After 20 days the ratio NO_x/NO_y for case 3 reaches 0.42, more than twice that for the other cases; 85% of the NO_x is in the form of NO for case 3 as compared with 33% under more typical conditions.

The partitioning of the Cl_x family is shown in Figures 4*c* (ClO) and 4*d* ($ClONO_2$). The initial perturbations to ClO are large, resulting in mixing ratios as much as a factor of 50 greater than steady state (55 ppt). Abundances decline as ClO is converted rapidly into $ClONO_2$ and more slowly into HCl by the reaction of Cl and CH_4. In our minimal case of heterogeneous processing (case 1), when only the partitioning within families is perturbed, ClO levels fall rapidly from 2.5 ppb to 0.2 ppb in the first 8 days; $ClONO_2$ increases to 1.9 ppb, becoming the dominant chlorine reservoir. Thereafter, the concentrations of both ClO and $ClONO_2$ decay slowly to the steady state limit, with time constants of 10-20 days, as both are converted into HCl.

When denitrification occurs (case 2), $ClONO_2$ becomes a less significant reservoir for chlorine during the first 20 days, and the recovery of ClO is limited by formation of HCl. Moreover, the steady state levels of ClO in the lower stratosphere are strongly and nonlinearly dependent on the relative abundances of Cl_x and NO_y: for example, in case 2 the decrease of NO_y from 8 to 2 ppb (factor of 4) increases the steady state mixing ratio of ClO from 55 to 335 ppt (factor of 6). The concurrent dehydration does not contribute to this increase in ClO; reducing H_2O levels by a factor of 4 decreases OH concentrations by only 10% and acts in the opposite sense to reduce ClO levels by shifting chlorine into the HCl reservoir.

When ozone concentrations are reduced by a factor of 10 (case 3), the chemical evolution is unusual, as above noted for NO_x. For the first 4 days the decay of ClO and the rise of $ClONO_2$ in Figures 4*a* and 4*b* look similar to cases 1 and 2. Thereafter, when NO_x levels reach a critical threshold, the chemical system becomes highly nonlinear and the Cl-ClO-$ClONO_2$ partitioning shifts dramatically in favor of Cl [see *Prather et al.*, 1979]. As a consequence, formation of HCl proceeds rapidly and a new steady state is reached in which the abundances of ClO (10 ppt) and $ClONO_2$ (38 ppt) are a factor of 30 less than the equivalent case 2. Thus with substantial ozone loss the chlorine cycle is effectively shut down at mid-latitudes, and the impact of chemical perturbations disappears rapidly.

What are the critical factors controlling ozone loss and residual perturbations to the chemistry of the mid-latitude stratosphere? Ozone loss is most rapid when ClO concentrations remain greater than 1 ppb for several days following transport of parcels to mid-latitudes. ClO-catalyzed loss of ozone may be truncated if the period of isolation of the parcel is reduced by a more rapid rate of strain. A more important factor governing ClO abundances in these calculations is the amount of NO_y: denitrified air will sustain substantially greater concentrations of ClO within the parcel.

Let us assume that over Antarctica the NO_y levels including any denitrification have not changed during the past two decades, while total chlorine (Cl_x plus halocarbons) has more than doubled since 1960. Observations in the Antarctic stratosphere [*Polar Ozone Workshop*, 1988; *Winkler and Gaines*, 1989] have shown that most of the halocarbons have been oxidized and a major fraction of total chlorine is in the form of Cl_x. The expected trend in Cl_x should lead to rapid, nonlinear increases in the residual ClO of heterogeneously processed air as shown in Figure 5. When Cl_x levels exceed 1.5 ppb in the denitrified parcel (2 ppb NO_y) ClO abundances

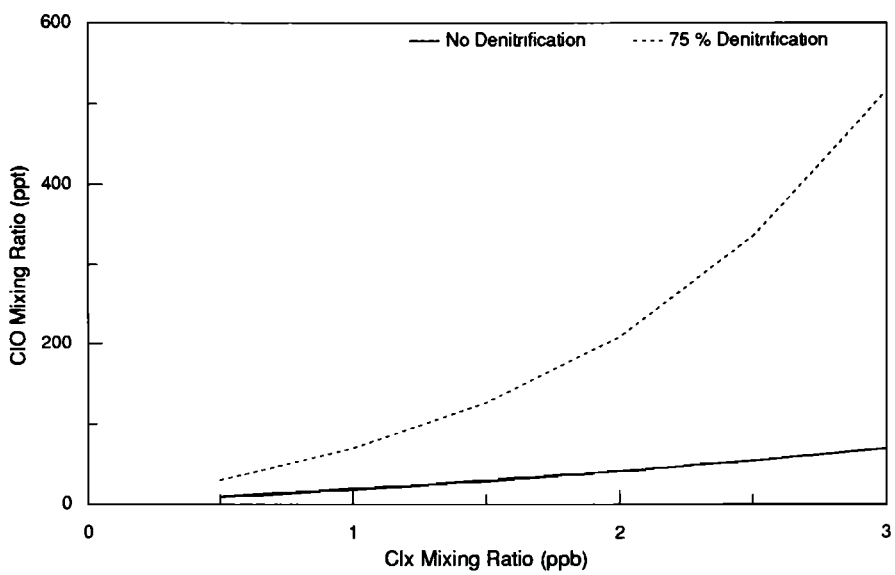

Fig. 5. Calculated steady state mixing ratios of ClO as a function of Cl_x in an air parcel moved from 75°S to 45°S at 20 km on November 1. The two curves correspond to unprocessed polar air (solid curve, cases 0-1) and denitrified/dehydrated air (dashed curve, case 2).

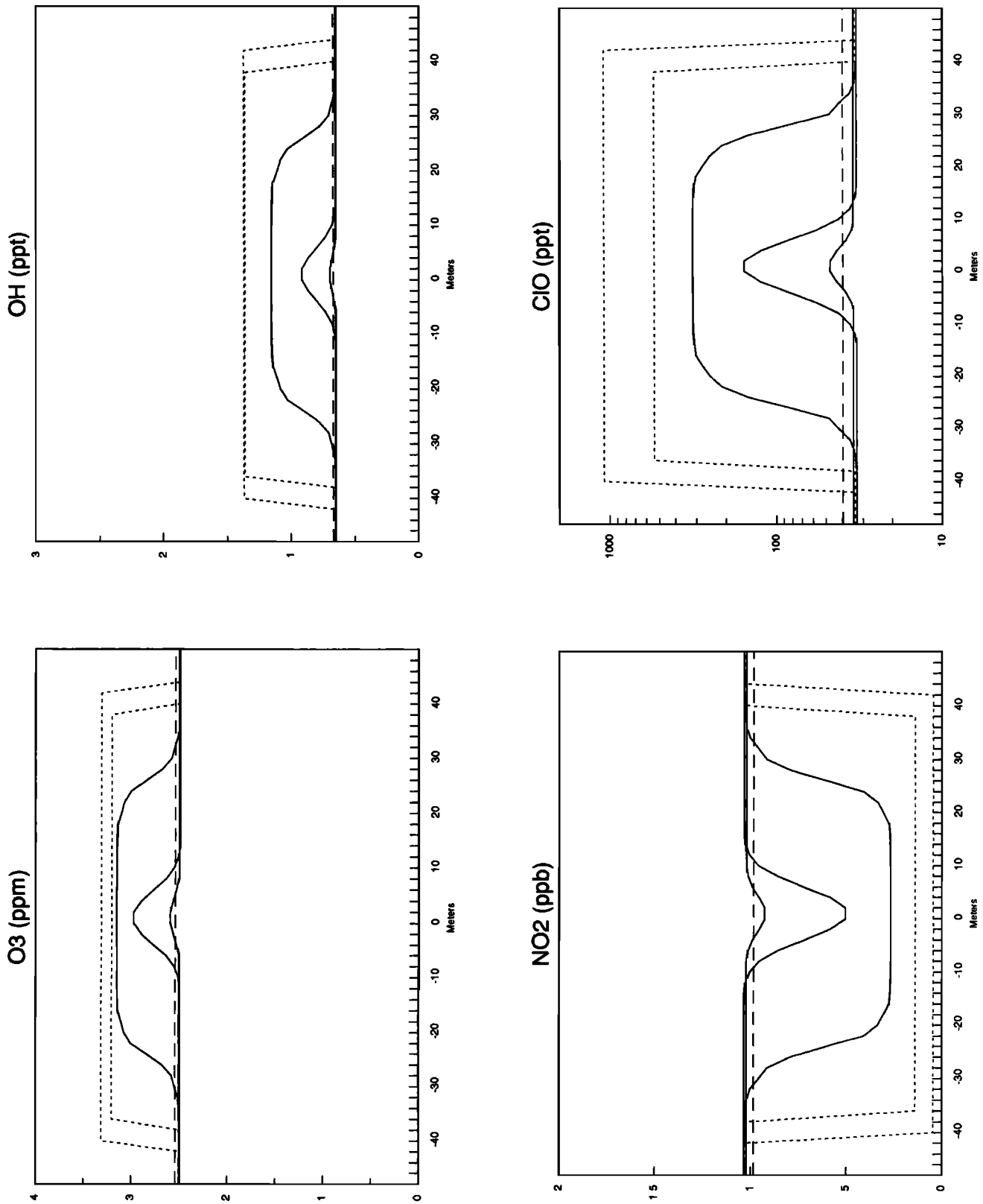
OH (ppt)
ClO (ppt)
O3 (ppm)
NO2 (ppb)
Meters

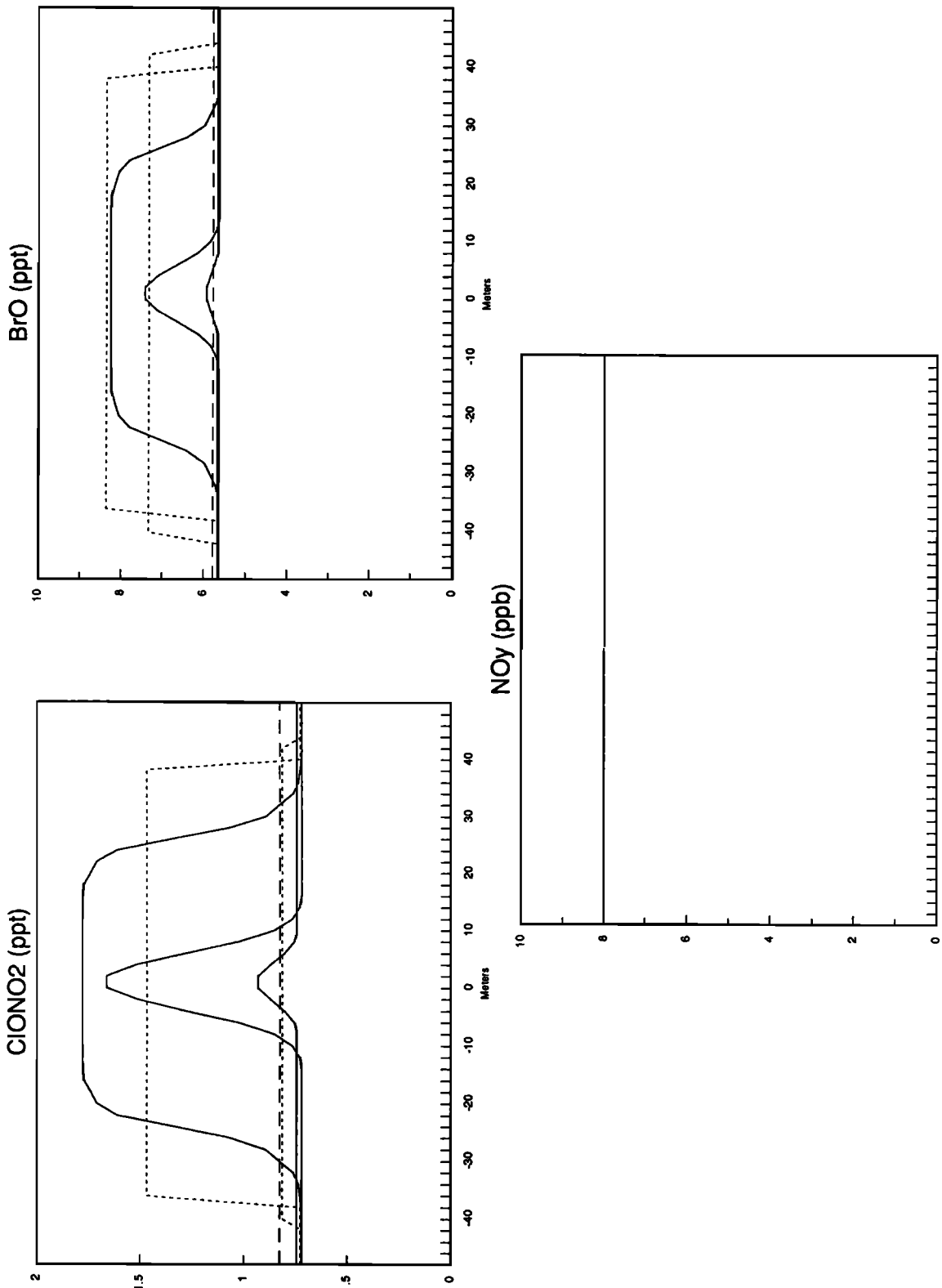

Fig. 6. Profiles of chemical species across a parcel of Antarctic air (case 1) as it mixes into the ambient atmosphere at 45°S, 20 km on November 1. The profiles are shown every 2 days, from days 2 to 12. Days 2 and 4 (dotted curve) have been compressed spatially for the purposes of display. Days 6, 8 and 10 are drawn as solid curves. At day 12 (dashed curve) the parcel is completely mixed. The computations are for case 1 (see text) and assume a diffusion coefficient $D = 3.5\ \mathrm{cm^2\ s^{-1}}$ and a strain rate $S = 10^{-5}\ \mathrm{s^{-1}}$.

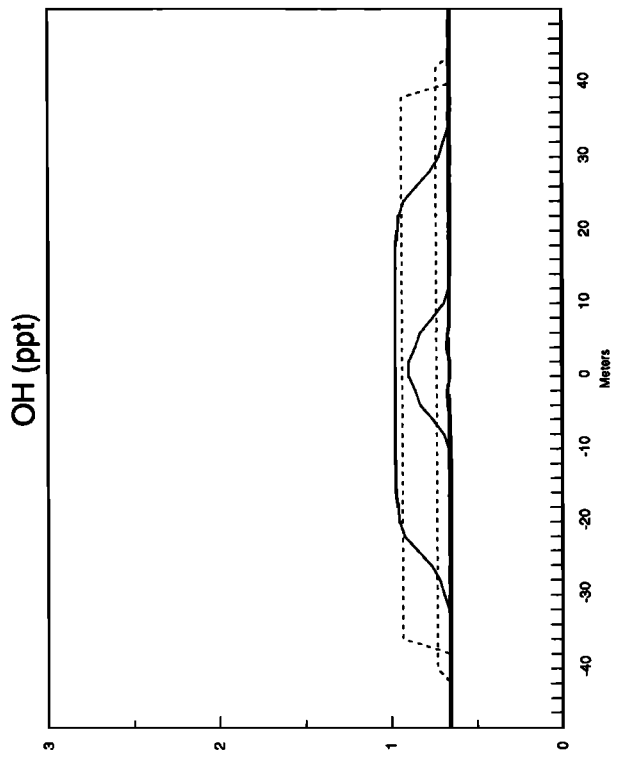
OH (ppt)
0
1
2
3
-40
-30
-20
-10
0
10
20
30
40
Meters

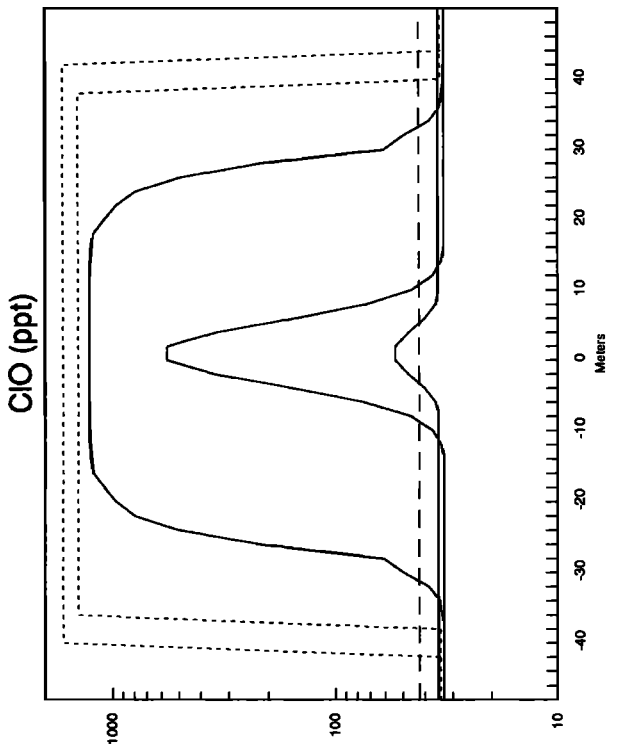
ClO (ppt)
10
100
1000
-40
-30
-20
-10
0
10
20
30
40
Meters

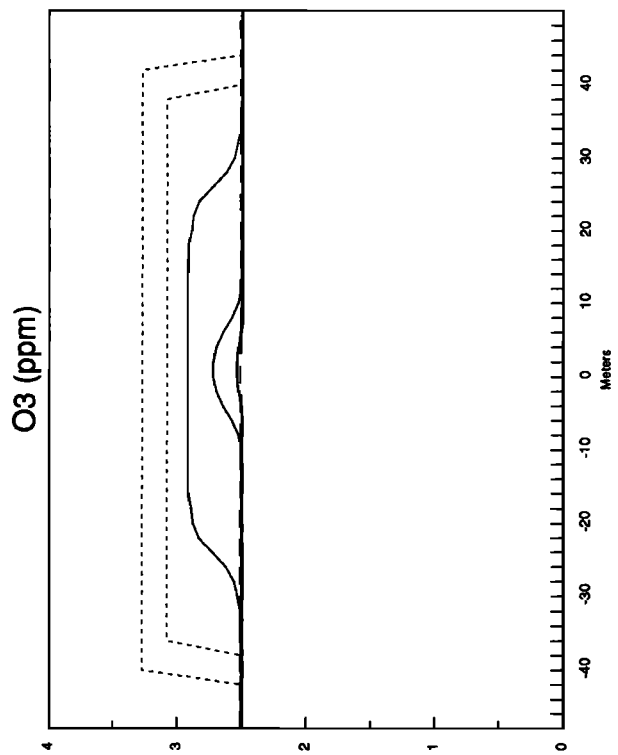
O3 (ppm)
0
1
2
3
4
-40
-30
-20
-10
0
10
20
30
40
Meters

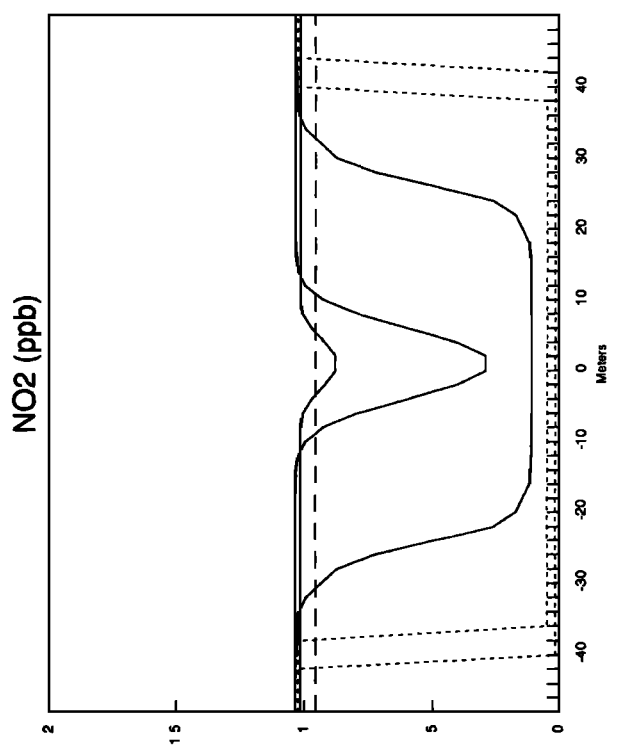
NO2 (ppb)
0
5
1
1.5
2
-40
-30
-20
-10
0
10
20
30
40
Meters

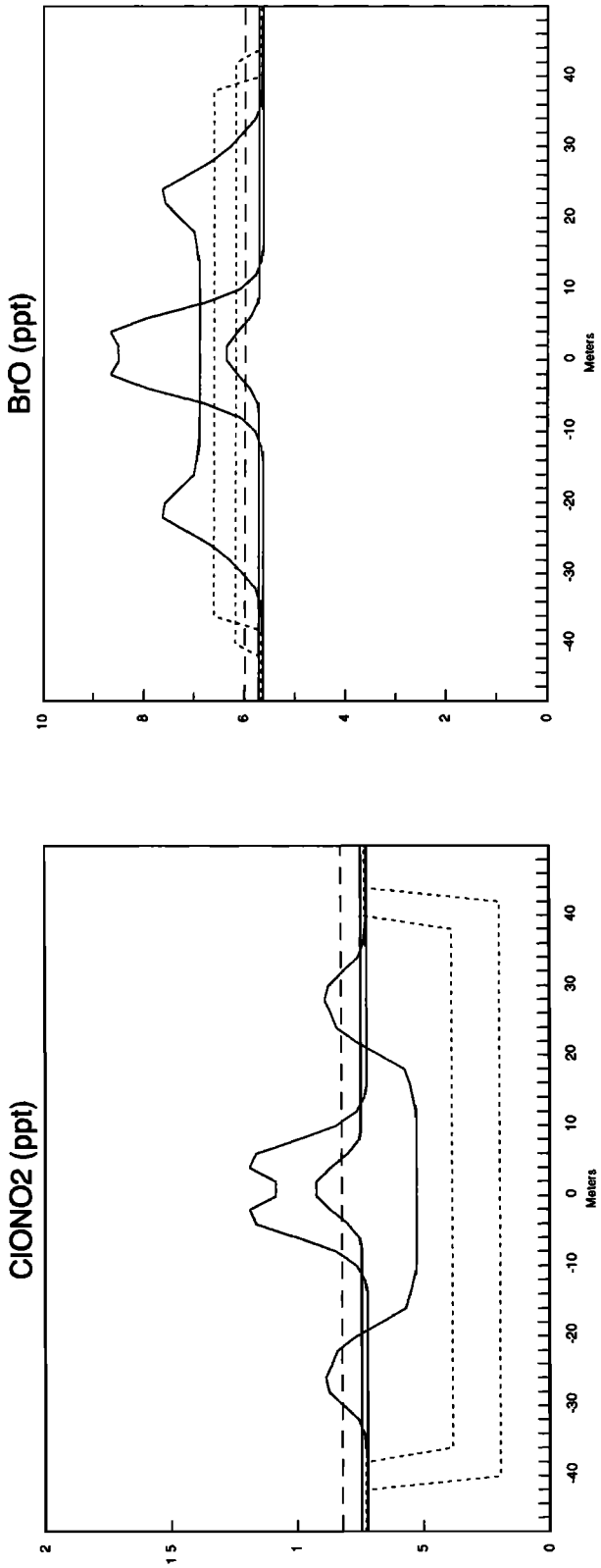

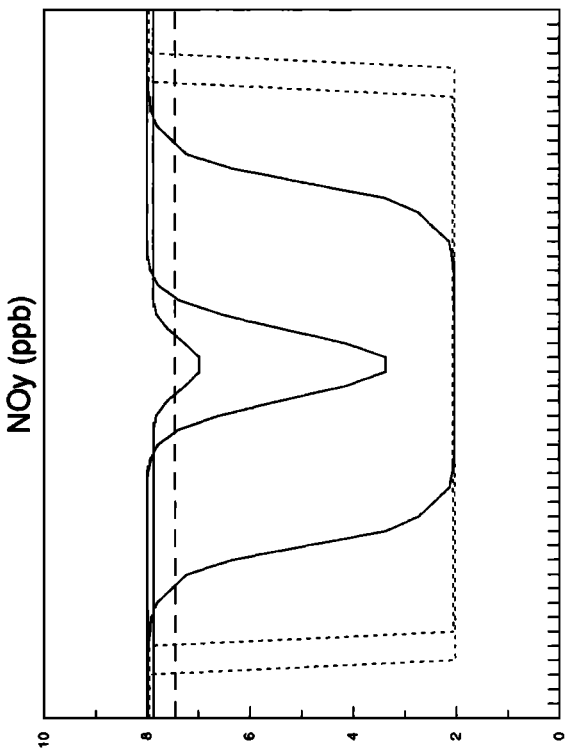

Fig. 7. Profiles of chemical species across a parcel of Antarctic air (case 2) as it mixes into the ambient atmosphere at 45°S, 20 km on November 1. See Figure 6.

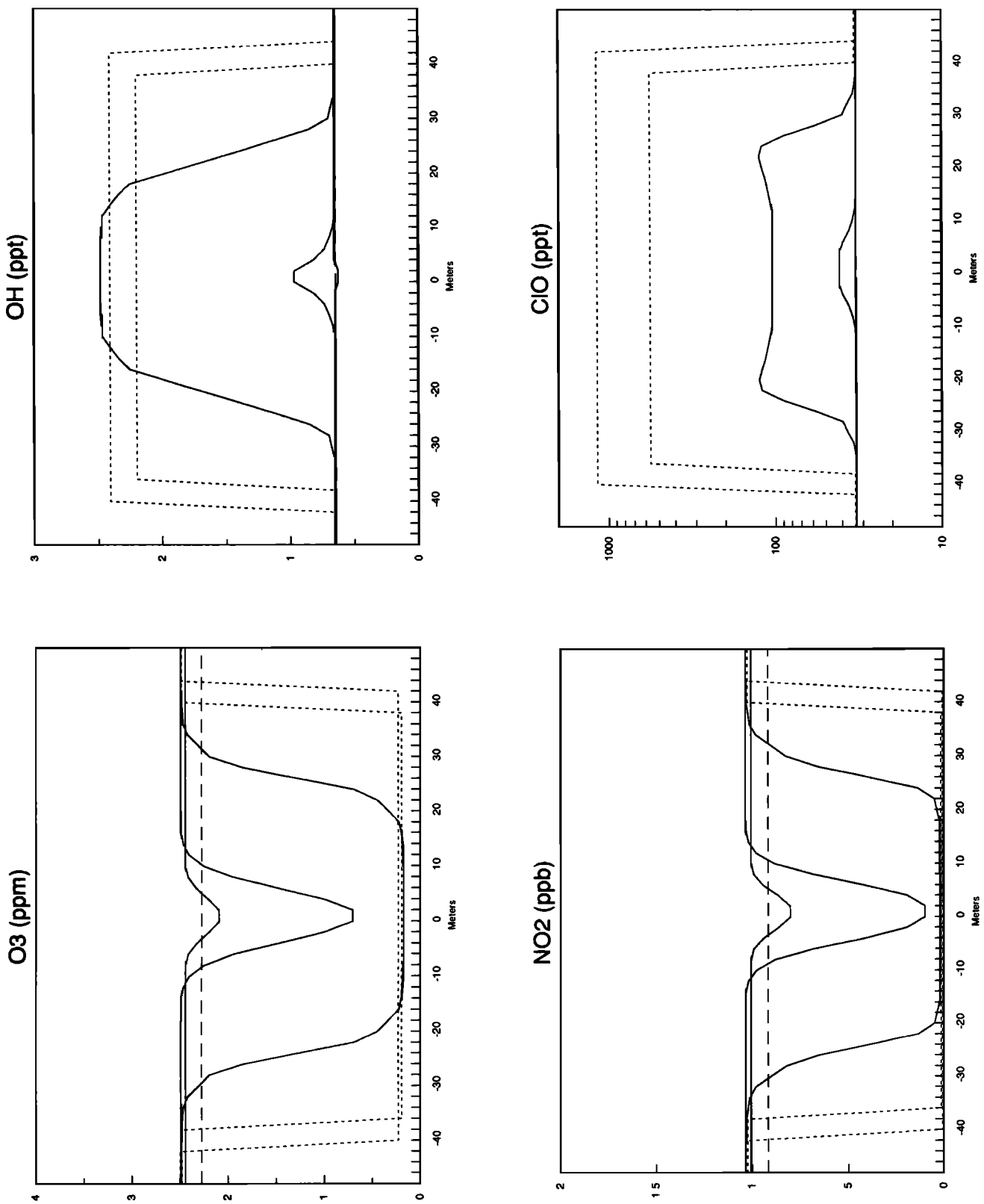
OH (ppt)
ClO (ppt)
O3 (ppm)
NO2 (ppb)
Meters

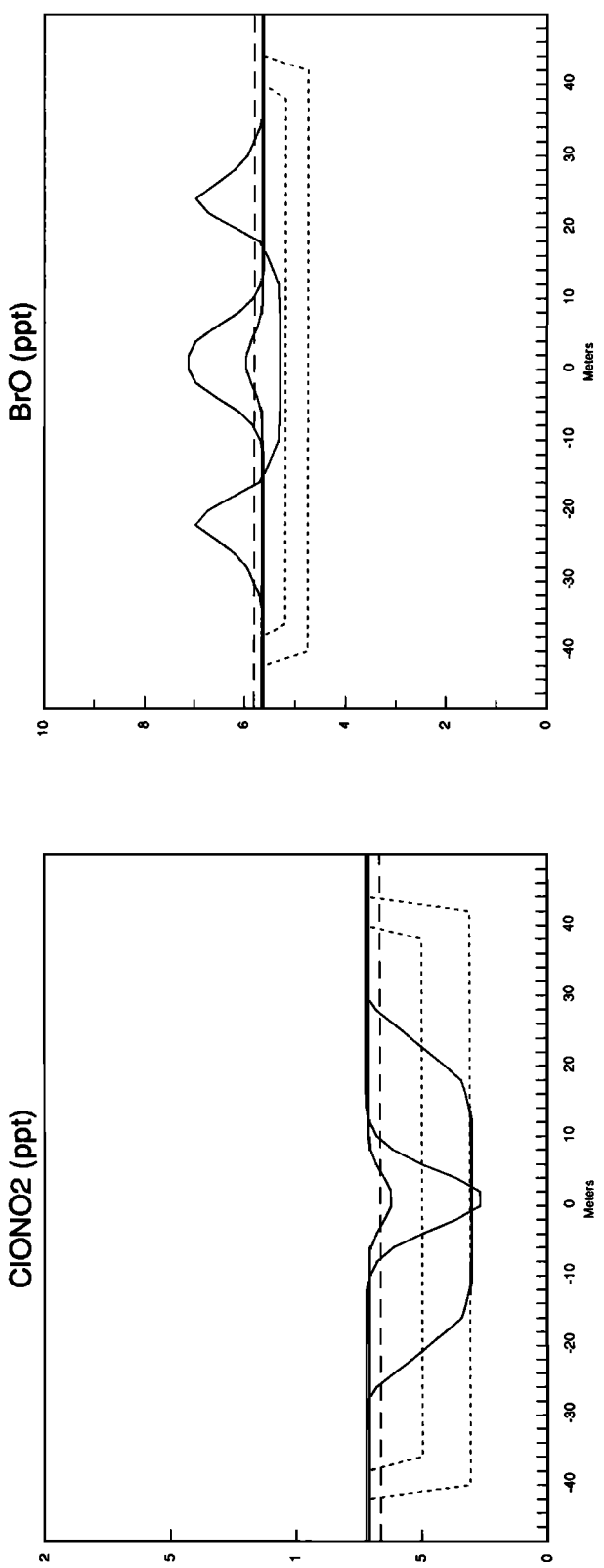

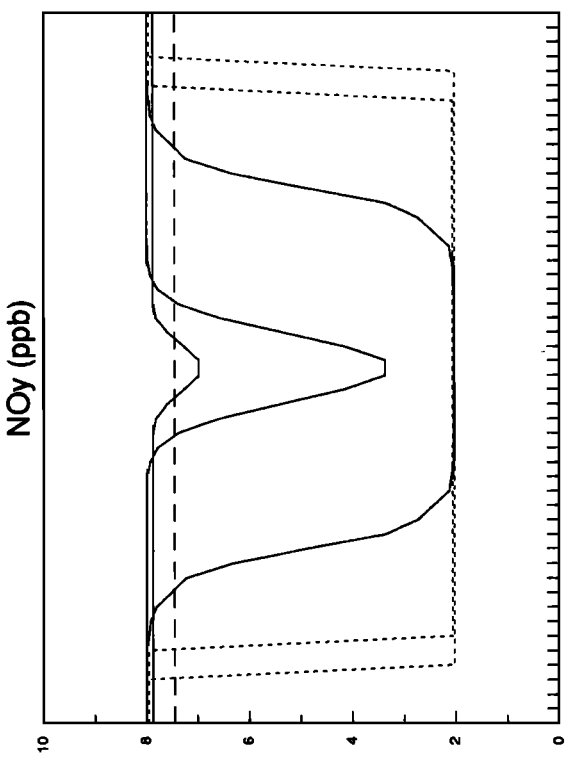

Fig. 8. Profiles of chemical species across a parcel of Antarctic air (case 3) as it mixes into the ambient atmosphere at 45°S, 20 km on November 1. See Figure 6.

increase dramatically; this effect occurs in air without denitrification (8 ppb NO_y) only when Cl_x concentrations exceed 6 ppb (not shown).

Ozone depletion associated with the transport of chemically perturbed air from the Antarctic to mid-latitudes will not be strongly influenced by the parcel's path (i.e., its history of latitudes and altitudes). When a parcel remains at 65°S (instead of 45°S as shown above), the perturbations to ClO take longer to decay, the colder temperatures increase loss from the dimer cycle, and thus ozone loss relative to the control at this latitude is about 10% greater after 10 days. Similarly, when the parcel evolves at lower altitudes, chemical recovery is slower and ozone loss is once again slightly greater. At higher altitudes, such as 24 km, photochemical recovery of NO_x is more rapid, ClO concentrations decrease correspondingly, and the relative ozone depletion is about 2/3 of that at 20 km. Dynamical considerations may overshadow these small differences in chemical evolution since, for example, parcels remaining near the edge of the polar vortex (65°S) will experience much greater wind shear and possibly be mixed more rapidly.

3.4. *Chemical Fronts*

The chemistry-strain-diffusion model combines strain and diffusion (equations (2) and (4)) with photochemistry (equation (5)) by splitting their respective operations. The time step is governed by the chemical package, and the strain-diffusion calculation is applied after each chemical time step, separately to each species across the entire grid. For most of the calculations shown below, the diffusion coefficient D is set to 3.5 $cm^2\ s^{-1}$, independent of species. We recognize that molecular diffusion results in larger species diffusing more slowly and, in one case, set $D = 1.0\ cm^2\ s^{-1}$ for HNO_3, $ClONO_2$, $BrONO_2$ and other species denoted by an asterisk in Table 1.

The calculations are set up in one dimension across the minimum thickness of the parcel, presumably the vertical dimension at the start. The one-dimensional grid is initialized with a parcel of heterogeneously processed polar air occupying 5 boxes at one end of the grid (effectively "doubled" to 9 boxes by the mirroring of the zero-flux boundary conditions) and with ambient mid-latitude air in the remaining 45 boxes. The parcel is followed from the initial size (10^3 m per grid box) until the mixing is complete (<1 m per grid box). Through the choice of boundary conditions and initial partitioning, the modeled domain maintains an average composition that is equivalent to an 89-to-9 mix of ambient-to-perturbed air. The initial, kilometer-thick layer would have significant gradients from top to bottom in photolysis rates and chemical composition; however, we focus here on the evolution and mixing of that air originating and remaining near 20 km (i.e., no substantial diabatic heating) and calculate the entire chemical evolution of the parcel for conditions at that altitude.

One expects to see a complex chemistry develop at the boundary between the ambient air and the polar air. High levels of ClO diffusing outward from the chemically perturbed polar air parcel should encounter ambient levels of NO_2 and O_3 diffusing inward. At this interface therefore production of $ClONO_2$ should rapidly rise. Furthermore, ozone destruction would be enhanced on one side of the interface by the outward diffusion of high levels of ClO but diminished on the other side by the erosion of ClO within the parcel. These effects occur, as discussed below, but are greatly suppressed by the action of atmospheric strain that continuously compresses the diffusion boundary.

The observable signatures of this chemical interface are shown in Figures 6–8 for cases 1–3. The abundance of NO_y, a conservative tracer here, maintains a sharp gradient (cases 2 and 3) until day 6 when diffusive mixing across the interface is first apparent; spatial structure disappears by day 12. Chemically active species evolve in isolation (as per Figure 4) until day 6; observable changes in the parcel during the early period are driven predominantly by chemistry. Thereafter the chemical front becomes identifiable. Diffusive mixing dominates after day 8, and the concentrations evolve rapidly as the parcel is finally dispersed into the ambient air.

Certain species exhibit unique, nonlinear behavior at the diffusive interface in cases 2 and 3. Both $ClONO_2$ (case 2) and BrO (cases 2 and 3) show a sharp peak in concentration at the boundary, visible only about days 6–8, when both diffusion and chemistry are active at the interface. For $ClONO_2$, this peak can be a factor of 2 greater than the abundances on either side. The buildup of $ClONO_2$ and BrO at the interface is temporary; the excess is returned to other reservoir species when the parcel finally disperses.

ClO concentrations within the parcel are as much as 50 times greater than ambient, and the final mixing of the parcel does not convert all of this excess into other chlorine reservoirs. Depending on the degree of initial heterogeneous processing, the level of ClO remaining throughout the model domain is as much as a factor of 5 greater than the ambient steady state concentration. The high levels of ClO persist through the final mixing because the time scale for conversion to HCl through Cl is slow, of order 20–60 days. At higher latitudes the conversion is slower, and enhanced levels of ClO may last into summer.

The spatial scale in Figures 6-8 corresponds to the thinnest dimension, presumably the vertical direction in the stratosphere as discussed above. Horizontal scales would likely be larger, but a clearly defined parcel extent of 5000 m on an isentropic surface is unlikely to be found for ribbon thicknesses of 50 m. The finest resolution offered by chemical measurements is about 200 m (1 Hz data from the ER–2), which would have difficulty resolving these chemical fronts unless the airplane path tracks along the ribbon of the deformed air parcel.

Molecular diffusion does not conserve family abundances if there are sharp gradients among the individual species. When we include the effects of differential rates of molecular diffusion in our calculations, the abundances of the families NO_y, Cl_x and Br_x tend to accumulate on one side of the chemical interface as shown in Figure 9 (for case 2). If a predominant reservoir of the chemical family on one side of the interface is a large, slowly diffusing molecule and a small, rapidly diffusing species on the other side, then the family abundance will accumulate on the side of the more slowly diffusing reservoir. For example, the Cl_x that builds up in certain regions, particularly those with initially high $ClONO_2$, will be chemically repartitioned thus further enhancing the abundance of $ClONO_2$ in this region relative to the case with uniform diffusion (compare Figures 7 and 9). The effects of differential diffusion in these calculations are small, and the

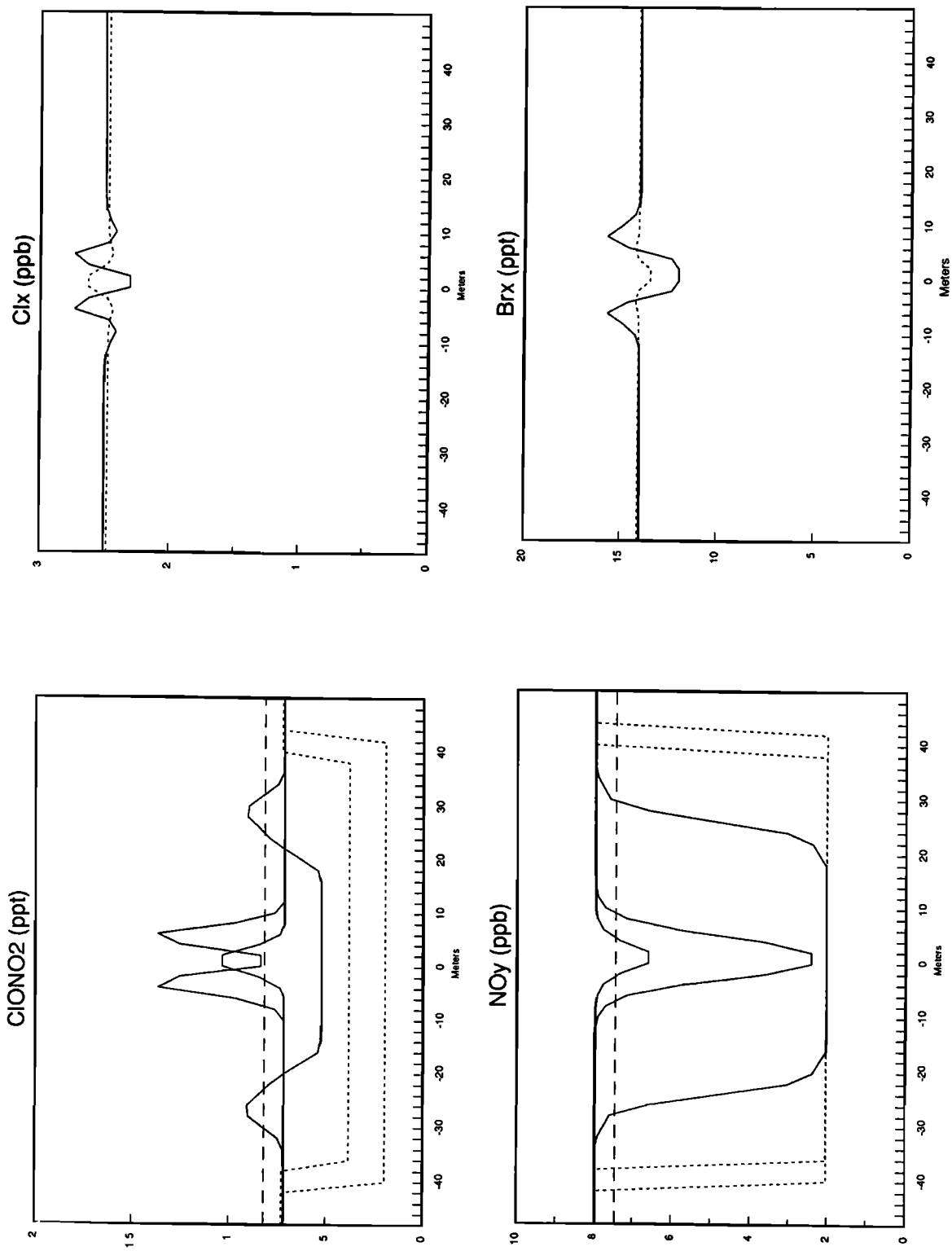

Fig. 9. Profiles of chemical species across a parcel of Antarctic air (case 2) as it mixes into the ambient atmosphere at 45°S, 20 km on November 1. The computation is similar to that shown in Figure 7, except that larger molecules (see Table 1) diffuse more slowly (D = 1.0 cm^2 s^{-1}). The profiles of $ClONO_2$ and NO_y are shown every 2 days, from day 2 to 12; profiles of Cl_x and Br_x are shown for days 8 (solid) and 10 (dashed). Note that variations in NO_y due to the slowly diffusing molecules are not readily apparent due to the factor of 4 difference in NO_y mixing ratio between the parcel and the ambient air. See Figure 6.

results are not changed substantially. The clumping of Cl_x and Br_x abundances is short-lived since the diffusion which creates it also rapidly destroys it.

An obvious residual effect on mid-latitude chemistry after the final mixing of the Antarctic parcels is the enhanced concentration of ClO, which may be as large as 5 times ambient. The impact of elevated levels of ClO will be to deplete ozone through reaction with BrO and to depress concentrations of NO_x through formation of $ClONO_2$. Compared with the control case in which unprocessed Antarctic air is mixed into the mid-latitudes, all three cases with heterogeneous processing begin with lower concentrations of NO_2. The reduced NO_2 abundances are a consequence of the denitrification of Antarctic air (cases 2 and 3) and, to a lesser extent, of different partitioning in the NO_y family; these reductions result in less ozone loss throughout the following season by the NO_x-catalytic cycle.

The budgets for odd oxygen, during the 12 days of mixdown and for the following 3 months, are summarized in Tables 2 and 3. For the control case 0, Table 2 gives a breakdown of all reactions that contribute to O_x production and loss in the lower mid-latitude stratosphere. Some reactions involving NO_y species may be thought of as producing O_x in that they lead to higher oxidation states of NO without consumption of O_x (e.g., $HO_2 + NO \rightarrow OH + NO_2$); we have grouped these reactions in Tables 2 and 3 as negative terms under net NO_x-cycle losses. The NO_x- and HO_x-catalytic cycles comprise most of the loss (33% and 40%, respectively), but the Chapman mechanism ($O + O_3 \rightarrow O_2 + O_2$) and the halogen cycles are also important. Loss exceeds production by about 25%, and ozone decreases by approximately 1.5 ppb per day.

Table 3 summarizes the evolution of O_3 and the O_x budget for the four test cases in the season following the final mixing. In cases 1 and 2 the largest loss of O_3 relative to the control occurs during the isolation period (the first 12 days), thereafter O_3 increases relative to the control. (All cases, including the control, show continued ozone loss throughout this period.) In case 3 the originally assumed ozone depletion (90% in the Antarctic parcel, resulting in a 12% decrease after complete mixing) shows enhanced recovery relative to the control, with only a 9% depletion at the end of the following season. The largest factor in this photochemical recovery is the reduced NO_x-cycle loss.

Polar denitrification and heterogenous processing play an important role in the ozone budget of the lower stratosphere at mid-latitudes, beyond that associated with the creation of the ozone hole itself and its subsequent transport to mid-latitudes. In the cases studied here, after complete mixing the perturbed chemistry acts to increase ozone, predominantly through reductions in NO_x-catalyzed loss. In the decades before the recent buildup of stratospheric chlorine, this processing of the Antarctic vortex would have made small contributions (<10%) to the abundance of ozone in the southern mid-latitude stratosphere.

TABLE 2. Odd Oxygen Catalytic Cycles

Reaction	Multiplier	90-Day Average, ppb/day	
$O+O_3 \rightarrow O_2+O_2$	×2	0.440	
$O(^1D)+O_3 \rightarrow O_2+O_2$	×2	0.050	
$O(^1D)+H_2O \rightarrow OH+OH$	×1	0.073	
$O(^1D)+CH_4 \rightarrow$ Products	×1	0.010	
O_x-cycle loss			0.573
$O+NO_2 \rightarrow NO+O_2$	×2	3.007	
$NO_3+h\nu \rightarrow NO+O_2$	×2	0.659	
$HO_2+NO \rightarrow OH+NO_2$	×(-1)	-1.386	
$CH_3OO+NO \rightarrow CH_3O+NO_2$	×(-1)	-0.059	
$HNO_3+OH \rightarrow H_2O+NO_3$	×(-1)	-0.052	
$HNO_4+h\nu \rightarrow OH+NO_3$	×(-1)	-0.076	
NO_x-cycle loss			2.093
$O_3+OH \rightarrow HO_2+O_2$	×1	1.904	
$O_3+HO_2 \rightarrow OH+O_2+O_2$	×1	0.528	
$O+OH \rightarrow O_2+H$	×1	0.002	
$O+HO_2 \rightarrow OH+O_2$	×1	0.022	
HO_x-cycle loss			2.456
$ClO+O \rightarrow Cl+O_2$	×2	0.297	
$HOCl+h\nu \rightarrow OH+Cl$	×1	0.071	
$Cl_2O_2+h\nu \rightarrow Cl+Cl+O_2$	×2	0.013	
$ClO+BrO \rightarrow BrCl+O_2$	×2	0.309	
$ClO+BrO \rightarrow Br+Cl+O_2$	×2	0.193	
$BrO+O \rightarrow Br+O_2$	×2	0.039	
$BrO+BrO \rightarrow Br+Br+O_2$	×2	0.017	
$HOBr+h\nu \rightarrow Br+OH$	×1	0.005	
Halogen-cycle loss			0.944
Total loss (all cycles)			6.066
$O_2+h\nu \rightarrow O+O$	×2	4.551	
Net loss minus production			1.515

At 20 km altitude 45°S November. Ozone mixing ratios averaged 2.51 ppm over the 90 day integration. Evolution of air consisting of an 89:9 mix of mid-latitude to Antarctic air (no heterogeneous processing; case 0 in text). Values are averaged over 90 days following final mixing on day number 12 (day numbers 13-102). Throughout this table, O refers to the ground state $O(^3P)$.

TABLE 3. Ozone Loss for Mixtures of Antarctic and Mid-latitude Air

	Ozone, ppm			
Day	Case 0	Case 1	Case 2	Case 3
0	2.592	2.592	2.592	2.303
12 (complete mixing)	2.587	2.540	2.512	2.274
50	2.507	2.465	2.442	2.246
102	2.453	2.416	2.397	2.228
ΔO_3 (0-12 days)	-0.005	-0.052	-0.080	-0.029
ΔO_3 (0-102 days)	-0.139	-0.176	-0.195	-0.075
	Rate, ppb/day			
Average (Days 13-102)	Case 0	Case 1	Case 2	Case 3
Production	4.55	4.55	4.55	4.55
O_x-cycle loss	0.57	0.56	0.55	0.47
NO_x-cycle loss	2.09	2.03	1.76	1.58
HO_x-cycle loss	2.46	2.42	2.48	2.18
Halogen-cycle loss	0.95	0.95	1.07	0.86
Net Loss	1.52	1.41	1.31	0.54

At 20 km 45°S November.

Therefore following the breakup of the polar vortex, chemical propagation of the Antarctic ozone hole occurs in two phases: rapid loss of ozone in the heterogeneously processed parcels as they evolve in isolation; and slower relative recovery of ozone over the following months. In the case of Antarctic air which has not experienced substantial ozone loss, chemical propagation generates an ozone deficit at mid-latitudes. In air that has already been depleted of ozone within the Antarctic vortex, chemical propagation acts in the opposite sense and can partially offset the deficit at mid-latitudes caused by dynamical dilution of the ozone hole.

4. Implications for Global Ozone

The model for strain and diffusion presented here makes predictions about the size distribution of chemically coherent air parcels in the stratosphere that can be tested by observation. The primary uncertainty in this model is the strain rate. Fundamental information on strain and mixing in the stratosphere may be obtained, ideally, by an observational analogue to the numerical experiments of *Juckes and McIntyre* [1987]. Analysis of potential vorticity maps on isentropic surfaces might provide a measure of the initial strain rate for large parcels but would be limited by the accurate spatial resolution of potential vorticity in the assimilated wind fields. The Airborne Antarctic Ozone Experiment has made extensive chemical and meteorological measurements in the Antarctic stratosphere with high spatial resolution [for example: *Anderson et al.*, 1989; *Fahey et al.*, 1989; *Lowenstein et al.*, 1989; *Tuck et al.*, 1989]. Analysis of the AAOE data set [*Winkler and Gaines*, 1989], especially in the chemically heterogeneous region just outside the vortex, should provide information about the sizes of distinct air parcels and their rates of mixing.

How large a chemical perturbation occurs at mid-latitudes when heterogeneously processed air from over Antarctica is finally mixed into the background stratosphere? Based on these calculations we expect the Antarctic air to remain isolated for 7–20 days following its separation from the vortex and to mix rapidly and completely within 30 days. The volume of Antarctic air is small (<10% of the southern hemisphere), but the impact on the mid-latitude stratosphere could still be large, depending on the amount of denitrification, enhancement of ClO and, of course, Antarctic ozone loss. In the case where denitrification occurs without ozone loss, ClO concentrations remain a factor of 5 above ambient levels after dilution. Return of ClO to ambient levels is determined by the time to reform HCl, 20 to 60 days depending on latitude. This mechanism may explain the high ClO values observed by *Brune et al.* [1988] well outside the polar vortex at 60°N in February 1988.

We have shown that following the breakup of the polar vortex, Antarctic air with substantially depleted O_3 (case 3) will not contribute any additional ozone loss at mid-latitudes as it is mixed with ambient air. These results support the three-dimensional simulations of the Antarctic ozone hole [*Prather et al.*, 1990] in which the hole was represented solely as an ozone deficit with the chemistry otherwise unperturbed. Nevertheless, air processed by PSCs, but transported to mid-latitudes before substantive ozone depletion, can lead to additional loss after mixing with ambient air. This latter effect is an important component needed in global simulations of the effects of polar chemistry on stratospheric ozone.

A simple extension of these results to the northern hemisphere would take into account that substantial Arctic ozone loss has not yet been observed. The occurrence of major heterogeneous processing by polar stratospheric clouds has not yet been demonstrated for the Arctic stratosphere, although there are preliminary indications of such [*Brune et al.*, 1988; *Solomon et al.*, 1988; *Mount et al.*, 1988]. Under these conditions, the propagation of chemically perturbed air may lead to spatially extensive loss of ozone of order few percent over northern mid-latitudes at the end of winter. This additional depletion may explain the discrepancy between the observed changes in column ozone (approximately −5% at 45°N winter from 1969 to 1986) and the predictions of global models (−2%), as discussed by the International Ozone Trends Panel [see *Watson et al.*, 1988]. Further analysis awaits publication of results from the Airborne Arctic Stratospheric Expedition of 1989 and incorporation of these effects into global models.

Fundamentally, the heterogeneous chemistry in the winter stratosphere is necessary to initialize perturbations to stratospheric chemistry, but denitrification or corresponding increases in atmospheric chlorine that result in greater abundances of chlorine than odd nitrogen are necessary for extensive and sustained global effects outside of the Antarctic ozone hole.

Acknowledgments. We wish to thank M. E. McIntyre for instructive criticisms on stratospheric mixing. This research was supported by a National Science Foundation grant to Columbia University (NSF-ATM-86-06057) and by the Upper Atmosphere Research Branch of the National Aeronautics and Space Administration.

References

Anderson, J. G., W. H. Brune, M. J. Proffitt, W. Starr, and K. R. Chan, In situ observations of ClO in the Antarctic: Evidence for chlorine catalyzed destruction of ozone, paper presented at Polar Ozone Workshop, Snowmass, Colo., May 9-13, 1988.

Anderson, J. G., W. H. Brune, and M. H. Proffitt, Ozone destruction by chlorine radicals within the Antarctic vortex: The spatial and temporal evolution of ClO-O_3 anticorrelation based on in situ ER-2 data, *J. Geophys. Res.*, *94*, 11465-11479, 1989.

Batchelor, G. K., The effects of homogeneous turbulence on material and line surfaces, *Proc. R. Soc. London, Ser. A*, *213*, 349, 1952.

Batchelor, G. K., Small-scale variation of convected quantities like temperature in a turbulent fluid, part 1, General discussion and the case of small conductivity, *J. Fluid Mech.*, *5*, 113-133, 1959.

Brune, W. H., D. W. Toohey, J. G. Anderson, W. L. Starr, J. F. Vedder, and E. F. Danielsen, In situ northern mid-latitude observations of ClO, O_3, and BrO in the wintertime lower stratosphere, *Science*, *242*, 558-562, 1988.

Burkholder, J. B., Measurements of the ClO radical vibrational band intensity and the ClO + ClO + M reaction product, paper presented at Polar Ozone Workshop, Snowmass, Colo., May 9-13, 1988.

Chipperfield, M. P., and J. A. Pyle, Two-dimensional modelling of the Antarctic lower stratosphere, *Geophys. Res. Lett.*, *15*, 875-878, 1988.

Cox, R. A., and G. D. Hayman, The stability and photochemistry of dimers of the ClO radical and implications for Antarctic ozone depletion, *Nature*, *332*, 796-800, 1988.

DeMore, W. B., M. J. Molina, S. P. Sander, D. M. Golden, R. F. Hampson, M. J. Kurylo, C. J. Howard, and A. R. Ravishankara, Chemical kinetics and photochemical data for use in stratospheric modeling: Evaluation no. 8, NASA panel for data evaluation, *Publ. 87-41*, Jet Propul. Lab., Pasadena, Calif., 1987.

de Zafra, R. L., M. Jaramillo, A. Parrish, P. Solomon, B. Connor, and J. Barrett, High concentrations of chlorine monoxide at low altitudes in the Antarctic spring stratosphere: Diurnal variation, *Nature*, *329*, 408-411, 1987.

Douglass, A. R., and R. S. Stolarski, Impact of heterogeneous chemistry on Arctic ozone, *Geophys. Res. Lett.*, *16*, 131-134, 1989.

Fahey, D. W., K. K. Kelly, G. V. Ferry, L. R. Poole, J. C. Wilson, D. M. Murphy, M. Lowenstein, and K. R. Chan, In situ measurements of total reactive nitrogen, total water, and aerosol in a polar stratospheric cloud in the Antarctic, *J. Geophys. Res.*, *94*, 11299-11316, 1989.

Fang, T.-M., S. C. Wofsy, and A. Dalgarno, Opacity distribution functions and absorption in Schumann-Runge bands of molecular oxygen, *Planet. Space Sci.*, *22*, 413-425, 1974.

Farman, J. C., B. J. Gardiner, and J. D. Shanklin, Large losses of total ozone in Antarctica reveal seasonal ClO_x/NO_x interaction, *Nature*, *315*, 207-210, 1985.

Hamill, P., R. P. Turco, and O. B. Toon, On the growth of the nitric acid and sulfuric acid hydrates under stratospheric conditions, *J. Atmos. Chem.*, *7*, 287-315, 1988.

Hanson, D., and K. Mauersberger, Laboratory studies of the nitric acid trihydrate: Implications for the south polar stratosphere, *Geophys. Res. Lett.*, *15*, 855-858, 1988.

Hayman, G. D., J. M. Davies, and R. A. Cox, Kinetics of the reaction ClO + ClO → Products, and its potential relevance to Antarctic ozone, *Geophys. Res. Lett.*, *15*, 855-858, 1988.

Hofmann, D. J., J. W. Harder, S. R. Rolf, and J. M. Rosen, Balloon-borne observations of the development and vertical structure of the Antarctic ozone hole in 1986, *Nature*, *326*, 59-62, 1987.

Holton, J. R. *An Introduction to Dynamical Meteorolgy, 2d ed.*, pp. 36-38, Academic, San Diego, Calif., 1979.

Juckes, M. N., and M. E. McIntyre, A high-resolution one-layer model of breaking planetary waves in the stratosphere, *Nature*, *328*, 590-596, 1987.

Keys, J. G., P. V. Johnston, W. A. Matthews, and R. L. McKenzie, Stratospheric NO_2 and O_3 in Antarctica: Dynamic and chemically controlled variations, *Geophys. Res. Lett.*, *13*, 1260-1263, 1986.

Kraichnan, R. H., Convection of a passive scalar by a quasi-uniform random straining field, *J. Fluid Mech.*, *64*, 737-762, 1974.

Logan, J. A., M. J. Prather, S. C. Wofsy, and M. B. McElroy, Atmospheric chemistry: Response to human influence, *Philos. Trans. R. Soc. London, Ser. A*, *290*, 187-234, 1978.

Logan, J. A., M. J. Prather, S. C. Wofsy, and M. B. McElroy, Tropospheric chemistry: A global perspective, *J. Geophys. Res.*, *86*, 7210-7254, 1981.

Lowenstein, M., J. R. Podolske, K. R. Chan, and S. E. Strahan, Nitrous oxide as a dynamical tracer in the 1987 Airborne Antarctic Ozone Experiment, *J. Geophys. Res.*, *94*, 11,589-11,598, 1989.

Mason, E. A., and T. R. Marrero, The diffusion of atoms and molecules, in *Advances in Atomic and Molecular Physics*, *6*, edited by D. R. Bates and J. Esterman, Academic, San Diego, Calif., 1970.

McCormick, M. P., and C. R. Trepte, SAM II measurements of Antarctic PSCs and aerosols, *Geophys. Res. Lett.*, *13*, 1276-1279, 1986.

McElroy, M. B., and R. J. Salawitch, Changing composition of the global stratosphere, *Science*, *243*, 763-770, 1989.

McIntyre, M. E. On the Antarctic ozone hole, *J. Atmos. Terr. Phys.*, *51*, 29-43, 1988.

McPeters, R. D., D. F. Heath, and P. K. Bhartia, Average ozone profiles for 1979 from the Nimbus-7 SBUV instrument, *J. Geophys. Res.*, *89*, 5199-5214, 1984.

Molina, L. T., and M. J. Molina, Production of Cl_2O_2 by the self reaction of the ClO radical, *J. Phys. Chem.*, *91*, 433-436, 1986.

Molina, M. J., T.-L. Tso, L. T. Molina, and F. C.-Y. Wang, Antarctic stratospheric chemistry of chlorine nitrate, hydrogen chloride, and ice: Release of active chlorine, *Science*, *238*, 1253-1257, 1987.

Mount, G. H., S. Solomon, R. W. Sanders, R. O. Jakoubek, and A. L. Schmeltekopf, Observations of stratospheric NO_2 and O_3 at Thule, Greenland, *Science*, *242*, 555-558, 1988.

NASA–WMO, Atmospheric ozone 1985: Assesment of our understanding of the processes controlling its present distribution and change, World Meteorol. Organ., Geneva, *Global Ozone Res. Monit. Proj. Rep. 16*, 1986.

Polar Ozone Workshop, Proceedings of the Polar Ozone Workshop held in Snowmass, Colorado, 9-13 May 1988, *NASA Conf. Publ. 10014*, 1988.

Prather, M. J., Solution of the inhomogeneous Rayleigh scattering atmosphere, *Astrophys. J.*, *192*, 787-792, 1974

Prather, M. J., M. B. McElroy, S. C. Wofsy, and J. A. Logan, Stratospheric chemistry: Multiple solutions, *Geophys. Res. Lett.*, *6*, 163-164, 1979.

Prather, M. J., M. B. McElroy, and S. C. Wofsy, Reductions in ozone at high concentrations of stratospheric halogens, *Nature*, *312*, 227-231, 1984.

Prather, M. J., M. M. Garcia, R. Suozzo, and D. Rind, Global impact of the Antarctic Ozone Hole: Dynamical dilution with a 3-D chemical transport model, *J. Geophys. Res.*, in press, 1990.

Salawitch, R. J., S. C. Wofsy, and M. B. McElroy, Influence of polar stratospheric clouds on the depletion of Antarctic ozone, *Geophys. Res. Lett.*, *15*, 871-874, 1988.

Sander, S. P., and R. R. Friedl, Kinetics and product studies of the BrO + ClO reaction: Implications for Antarctic chemistry, *Geophys. Res. Lett.*, *15*, 887-890, 1988.

Sander, S. P., R. R. Friedl, and Y. L Yung, Rate for formation of the ClO dimer in the polar stratosphere: Implications for ozone loss, *Science*, *245*, 1095-1098, 1989.

Solomon, S., G. H. Mount, R. W. Saunders, and A. L. Schmeltekopf, Visible spectroscopy at McMurdo Station, Antarctica, 2, Observations of OClO, *J. Geophys. Res.*, *92*, 8329-8338, 1987.

Solomon, S., G. H. Mount, R. W. Sanders, R. O. Jakoubek, and A. L. Schmeltekopf, Observations of the nighttime abundance of OClO in the winter stratosphere above Thule, Greenland, *Science*, *242*, 558-562, 1988.

Stolarski, R. S., A. J. Krueger, M. R. Schoeberl, R. D. McPeters, P. A. Newman, and J. C. Alpert, Nimbus 7 SBUV/TOMS measurements of the springtime Antarctic ozone hole, *Nature*, *322*, 808-811, 1986.

Sze, N. D., M. K. W. Ko, D. K. Weisenstein, J. M. Rodriguez, R. S. Stolarski, and M. R. Schoeberl, Antarctic ozone hole: Possible implications for ozone trends in the southern hemisphere, *J. Geophys. Res.*, *94*, 11,521-11,528, 1989.

Tolbert, M. A., M. J. Rossi, and D. M. Golden, Heterogeneous interactions of chlorine nitrate, hydrogen chloride, and nitric acid with sulfuric acid surfaces at stratospheric temperatures, *Geophys. Res. Lett.*, *15*, 847-850, 1988.

Toon, O. B., P. Hamill, R. P. Turco, and J. Pinto, Condensation of HNO_3 and HCl in the winter polar stratosphere, *Geophys. Res. Lett.*, *13*, 1284-1287, 1986.

Tuck, A. F., R. T. Watson, E. P. Condon, J. J. Margitan, and O. B. Toon, The planning and execution of ER-2 and DC-8 aircraft flights over Antarctica, August and September 1987, *J. Geophys. Res.*, *94*, 11,179-11,180, 1989.

Wahner, A., G. S. Tyndall, and A. R. Ravishankara, Absorption cross sections for OClO as a function of temperature in the wavelength range 240-480 nm, *J. Phys. Chem.*, *91*, 2734-2736, 1987.

Watson, R. T. and Ozone Trends Panel, M. J. Prather and Ad Hoc Theory Panel, and M. J. Kurylo and NASA Panel for Data Evaluation, Present state of knowledge of the upper atmosphere 1988: An assesment report, *NASA Ref. Publ. 1208*, 1988.

Welander, P., Studies on the general development of motion in a 2-D ideal fluid, *Tellus*, *7*, 141-156, 1955.

Winkler, R., and S. Gaines (Eds.), *Airborne Antarctic Ozone Experiment: September-August, 1987, UARP-CD-002*, NASA Upper Atmosphere Research Program, Washington, D.C., 1989.

Wofsy, S. C., M. J. Molina, R. J. Salawitch, L. E. Fox, and M. B. McElroy, Interactions between HCl, NO_x, and H_2O ice in the Antarctic stratosphere: Implications for ozone, *J. Geophys. Res.*, *93*, 2442-2450, 1988.

A. H. Jaffe, Department of Astronomy and Astrophysics, University of Chicago, Chicago, IL 60637.

M. J. Prather, NASA/GISS, 2880 Broadway, New York, NY 10025.

(Received June 12, 1989;
revised September 11, 1989;
accepted September 11, 1989.)